Published April 18, 2011

This work was supported by the Grant-in-Aid for Scientific Support Programs for Cancer Research; Grant-in-Aid for Scientific Research on Innovative Areas, and Ministry of Education, Culture, Sports, Science, and Technology of Japan (H. Tahara). This work was partially supported by the Science and Technology Incubation Program in Advanced Regions, Japan Science and Technology Agency, and Takeda Science Foundation (H. Tarara) and the Program for the Promotion of Fundamental Studies in Health Science of the National Institute of Biomedical Innovation (T. Ochiya).

Submitted: 20 October 2010
Accepted: 18 March 2011

References

Adams, P.D. 2007. Remodeling of chromatin structure in senescent cells and its potential impact on tumor suppression and aging. *Gene.* 397:84–93. doi:10.1016/j.gene.2007.04.020

Agirre, X., A. Jiménez-Velasco, E. San José-Enériz, L. Garate, E. Bandrés, L. Cordeu, O. Aparicio, B. Saez, G. Navarro, A. Vilas-Zornoza, et al. 2008. Down-regulation of hsa-miR-10a in chronic myeloid leukemia CD34+ cells increases USF2-mediated cell growth. *Mol. Cancer Res.* 6:1830–1840. doi:10.1158/1541-7786.MCR-08-0167

Akao, Y., Y. Nakagawa, and T. Naoe. 2006. let-7 microRNA functions as a potential growth suppressor in human colon cancer cells. *Biol. Pharm. Bull.* 29:903–906. doi:10.1248/bpb.29.903

Bar, N., and R. Dikstein. 2010. miR-22 forms a regulatory loop in PTEN/AKT pathway and modulates signaling kinetics. *PLoS ONE.* 5:e10859. doi:10.1371/journal.pone.0010859

Bartel, D.P. 2004. MicroRNAs: genomics, biogenesis, mechanism, and function. *Cell.* 116:281–297. doi:10.1016/S0092-8674(04)00045-5

Belguise, K., N. Kersual, F. Galtier, and D. Chalbos. 2005. FRA-1 expression level regulates proliferation and invasiveness of breast cancer cells. *Oncogene.* 24:1434–1444. doi:10.1038/sj.onc.1208312

Braig, M., S. Lee, C. Loddenkemper, C. Rudolph, A.H. Peters, B. Schlegelberger, H. Stein, B. Dörken, T. Jenuwein, and C.A. Schmitt. 2005. Oncogene-induced senescence as an initial barrier in lymphoma development. *Nature.* 436:660–665. doi:10.1038/nature03841

Brooks, C.L., and W. Gu. 2009. How does SIRT1 affect metabolism, senescence and cancer? *Nat. Rev. Cancer.* 9:123–128. doi:10.1038/nrc2562

Calin, G.A., and C.M. Croce. 2006. MicroRNA signatures in human cancers. *Nat. Rev. Cancer.* 6:857–866. doi:10.1038/nrc1997

Calin, G.A., C. Sevignani, C.D. Dumitru, T. Hyslop, E. Noch, S. Yendamuri, M. Shimizu, S. Rattan, F. Bullrich, M. Negrini, and C.M. Croce. 2004. Human microRNA genes are frequently located at fragile sites and genomic regions involved in cancers. *Proc. Natl. Acad. Sci. USA.* 101:2999–3004. doi:10.1073/pnas.0307323101

Campisi, J. 2005. Senescent cells, tumor suppression, and organismal aging: good citizens, bad neighbors. *Cell.* 120:513–522. doi:10.1016/j.cell.2005.02.003

Chen, Q.M., V.C. Tu, J. Catania, M. Burton, O. Toussaint, and T. Dilley. 2000. Involvement of Rb family proteins, focal adhesion proteins and protein synthesis in senescent morphogenesis induced by hydrogen peroxide. *J. Cell Sci.* 113:4087–4097.

Chen, Y., Y. Song, Z. Wang, Z. Yue, H. Xu, C. Xing, and Z. Liu. 2010. Altered expression of MiR-148a and MiR-152 in gastrointestinal cancers and its clinical significance. *J. Gastrointest. Surg.* 14:1170–1179. doi:10.1007/s11605-010-1202-2

Choong, M.L., H.H. Yang, and I. McNiece. 2007. MicroRNA expression profiling during human cord blood-derived CD34 cell erythropoiesis. *Exp. Hematol.* 35:551–564. doi:10.1016/j.exphem.2006.12.002

Collado, M., J. Gil, A. Efeyan, C. Guerra, A.J. Schuhmacher, M. Barradas, A. Benguría, A. Zaballos, J.M. Flores, M. Barbacid, et al. 2005. Tumour biology: senescence in premalignant tumours. *Nature.* 436:642. doi:10.1038/436642a

Debacq-Chainiaux, F., J.D. Erusalimsky, J. Campisi, and O. Toussaint. 2009. Protocols to detect senescence-associated beta-galactosidase (SA-betagal) activity, a biomarker of senescent cells in culture and in vivo. *Nat. Protoc.* 4:1798–1806. doi:10.1038/nprot.2009.191

Deng, Y., S.S. Chan, and S. Chang. 2008. Telomere dysfunction and tumour suppression: the senescence connection. *Nat. Rev. Cancer.* 8:450–458. doi:10.1038/nrc2393

Díaz, R., J. Silva, J.M. García, Y. Lorenzo, V. García, C. Peña, R. Rodríguez, C. Muñoz, F. García, F. Bonilla, and G. Domínguez. 2008. Deregulated expression of miR-106a predicts survival in human colon cancer patients. *Genes Chromosomes Cancer.* 47:794–802. doi:10.1002/gcc.20580

Dimri, G.P., X. Lee, G. Basile, M. Acosta, G. Scott, C. Roskelley, E.E. Medrano, M. Linskens, I. Rubelj, O. Pereira-Smith, et al. 1995. A biomarker that identifies senescent human cells in culture and in aging skin in vivo. *Proc. Natl. Acad. Sci. USA.* 92:9363–9367. doi:10.1073/pnas.92.20.9363

Elmén, J., M. Lindow, A. Silahtaroglu, M. Bak, M. Christensen, A. Lind-Thomsen, M. Hedtjärn, J.B. Hansen, H.F. Hansen, E.M. Straarup, et al. 2008. Antagonism of microRNA-122 in mice by systemically administered LNA-antimiR leads to up-regulation of a large set of predicted target mRNAs in the liver. *Nucleic Acids Res.* 36:1153–1162. doi:10.1093/nar/gkm1113

Fabbri, M., R. Garzon, A. Cimmino, Z. Liu, N. Zanesi, E. Callegari, S. Liu, H. Alder, S. Costinean, C. Fernandez-Cymering, et al. 2007. MicroRNA-29 family reverts aberrant methylation in lung cancer by targeting DNA methyltransferases 3A and 3B. *Proc. Natl. Acad. Sci. USA.* 104:15805–15810. doi:10.1073/pnas.0707628104

Gangaraju, V.K., and H. Lin. 2009. MicroRNAs: key regulators of stem cells. *Nat. Rev. Mol. Cell Biol.* 10:116–125. doi:10.1038/nrm2621

Garofalo, M., and C.M. Croce. 2011. microRNAs: Master regulators as potential therapeutics in cancer. *Annu. Rev. Pharmacol. Toxicol.* 51:25–43. doi:10.1146/annurev-pharmtox-010510-100517

Haferkamp, S., S.L. Tran, T.M. Becker, L.L. Scurr, R.F. Kefford, and H. Rizos. 2009. The relative contributions of the p53 and pRb pathways in oncogene-induced melanocyte senescence. *Aging (Albany NY).* 1:542–556.

Hahn, W.C., and R.A. Weinberg. 2002. Rules for making human tumor cells. *N. Engl. J. Med.* 347:1593–1603. doi:10.1056/NEJMra021902

He, L., and G.J. Hannon. 2004. MicroRNAs: small RNAs with a big role in gene regulation. *Nat. Rev. Genet.* 5:522–531. doi:10.1038/nrg1379

Huang, J., Q. Gan, L. Han, J. Li, H. Zhang, Y. Sun, Z. Zhang, and T. Tong. 2008. SIRT1 overexpression antagonizes cellular senescence with activated ERK/S6k1 signaling in human diploid fibroblasts. *PLoS ONE.* 3:e1710.

Hummel, R., D.J. Hussey, and J. Haier. 2010. MicroRNAs: predictors and modifiers of chemo- and radiotherapy in different tumour types. *Eur. J. Cancer.* 46:298–311. doi:10.1016/j.ejca.2009.10.027

Ibarra, I., Y. Erlich, S.K. Muthuswamy, R. Sachidanandam, and G.J. Hannon. 2007. A role for microRNAs in maintenance of mouse mammary epithelial progenitor cells. *Genes Dev.* 21:3238–3243. doi:10.1101/gad.1616307

Iliopoulos, D., K.N. Malizos, P. Oikonomou, and A. Tsezou. 2008. Integrative microRNA and proteomic approaches identify novel osteoarthritis genes and their collaborative metabolic and inflammatory networks. *PLoS ONE.* 3:e3740. doi:10.1371/journal.pone.0003740

Jessel, R., S. Haertel, C. Socaciu, S. Tykhonova, and H.A. Diehl. 2002. Kinetics of apoptotic markers in exogeneously induced apoptosis of EL4 cells. *J. Cell. Mol. Med.* 6:82–92. doi:10.1111/j.1582-4934.2002.tb00313.x

Katakowski, M., X. Zheng, F. Jiang, T. Rogers, A. Szalad, and M. Chopp. 2010. MiR-146b-5p suppresses EGFR expression and reduces in vitro migration and invasion of glioma. *Cancer Invest.* 28:1024–1030. doi:10.3109/07357907.2010.512596

Kawahigashi, Y., T. Mishima, Y. Mizuguchi, Y. Arima, S. Yokomuro, T. Kanda, O. Ishibashi, H. Yoshida, T. Tajiri, and T. Takizawa. 2009. MicroRNA profiling of human intrahepatic cholangiocarcinoma cell lines reveals biliary epithelial cell-specific microRNAs. *J. Nippon Med. Sch.* 76:188–197. doi:10.1272/jnms.76.188

Kong, W., L. He, M. Coppola, J. Guo, N.N. Esposito, D. Coppola, and J.Q. Cheng. 2010. MicroRNA-155 regulates cell survival, growth, and chemosensitivity by targeting FOXO3a in breast cancer. *J. Biol. Chem.* 285:17869–17879. doi:10.1074/jbc.M110.101055

Kota, J., R.R. Chivukula, K.A. O'Donnell, E.A. Wentzel, C.L. Montgomery, H.W. Hwang, T.C. Chang, P. Vivekanandan, M. Torbenson, K.R. Clark, et al. 2009. Therapeutic microRNA delivery suppresses tumorigenesis in a murine liver cancer model. *Cell.* 137:1005–1017. doi:10.1016/j.cell.2009.04.021

Koutsodontis, G., I. Tentes, P. Papakosta, A. Moustakas, and D. Kardassis. 2001. Sp1 plays a critical role in the transcriptional activation of the human cyclin-dependent kinase inhibitor p21(WAF1/Cip1) gene by the p53 tumor suppressor protein. *J. Biol. Chem.* 276:29116–29125. doi:10.1074/jbc.M104130200

Lafferty-Whyte, K., C.J. Cairney, N.B. Jamieson, K.A. Oien, and W.N. Keith. 2009. Pathway analysis of senescence-associated miRNA targets reveals common processes to different senescence induction mechanisms. *Biochim. Biophys. Acta.* 1792:341–352.

Lee, Y.S., and A. Dutta. 2007. The tumor suppressor microRNA let-7 represses the HMGA2 oncogene. *Genes Dev.* 21:1025–1030. doi:10.1101/gad.1540407

Li, N., H. Fu, Y. Tie, Z. Hu, W. Kong, Y. Wu, and X. Zheng. 2009. miR-34a inhibits migration and invasion by down-regulation of c-Met expression in human hepatocellular carcinoma cells. *Cancer Lett.* 275:44–53. doi:10.1016/j.canlet.2008.09.035

Published April 18, 2011

Li, X., J. Liu, R. Zhou, S. Huang, S. Huang, and X.M. Chen. 2010. Gene silencing of MIR22 in acute lymphoblastic leukaemia involves histone modifications independent of promoter DNA methylation. *Br. J. Haematol.* 148:69–79. doi:10.1111/j.1365-2141.2009.07920.x

Liu, L., Y. Jiang, H. Zhang, A.R. Greenlee, R. Yu, and Q. Yang. 2010. miR-22 functions as a micro-oncogene in transformed human bronchial epithelial cells induced by anti-benzo[a]pyrene-7,8-diol-9,10-epoxide. *Toxicol. In Vitro.* 24:1168–1175. doi:10.1016/j.tiv.2010.02.016

Liu, Q., H. Fu, F. Sun, H. Zhang, Y. Tie, J. Zhu, R. Xing, Z. Sun, and X. Zheng. 2008. miR-16 family induces cell cycle arrest by regulating multiple cell cycle genes. *Nucleic Acids Res.* 36:5391–5404. doi:10.1093/nar/gkn522

Narita, M., and S.W. Lowe. 2005. Senescence comes of age. *Nat. Med.* 11:920–922. doi:10.1038/nm0905-920

Narita, M., S. Nũnez, E. Heard, M. Narita, A.W. Lin, S.A. Hearn, D.L. Spector, G.J. Hannon, and S.W. Lowe. 2003. Rb-mediated heterochromatin formation and silencing of E2F target genes during cellular senescence. *Cell.* 113:703–716. doi:10.1016/S0092-8674(03)00401-X

Neely, L.A., S. Patel, J. Garver, M. Gallo, M. Hackett, S. McLaughlin, M. Nadel, J. Harris, S. Gullans, and J. Rooke. 2006. A single-molecule method for the quantitation of microRNA gene expression. *Nat. Methods.* 3:41–46. doi:10.1038/nmeth825

Ohtani, N., D.J. Mann, and E. Hara. 2009. Cellular senescence: its role in tumor suppression and aging. *Cancer Sci.* 100:792–797. doi:10.1111/j.1349-7006.2009.01123.x

Ota, H., E. Tokunaga, K. Chang, M. Hikasa, K. Iijima, M. Eto, K. Kozaki, M. Akishita, Y. Ouchi, and M. Kaneki. 2006. Sirt1 inhibitor, Sirtinol, induces senescence-like growth arrest with attenuated Ras-MAPK signaling in human cancer cells. *Oncogene.* 25:176–185.

Pandey, D.P., and D. Picard. 2009. miR-22 inhibits estrogen signaling by directly targeting the estrogen receptor alpha mRNA. *Mol. Cell. Biol.* 29:3783–3790. doi:10.1128/MCB.01875-08

Poliseno, L., L. Pitto, M. Simili, L. Mariani, L. Riccardi, A. Ciucci, M. Rizzo, M. Evangelista, A. Mercatanti, P.P. Pandolfi, and G. Rainaldi. 2008. The proto-oncogene LRF is under post-transcriptional control of MiR-20a: implications for senescence. *PLoS ONE.* 3:e2542. doi:10.1371/journal.pone.0002542

Ricarte-Filho, J.C., C.S. Fuziwara, A.S. Yamashita, E. Rezende, M.J. da-Silva, and E.T. Kimura. 2009. Effects of let-7 microRNA on cell growth and differentiation of papillary thyroid cancer. *Transl Oncol.* 2:236–241.

Ruas, M., F. Gregory, R. Jones, R. Poolman, M. Starborg, J. Rowe, S. Brookes, and G. Peters. 2007. CDK4 and CDK6 delay senescence by kinase-dependent and p16INK4a-independent mechanisms. *Mol. Cell. Biol.* 27:4273–4282. doi:10.1128/MCB.02286-06

Schmitt, C.A. 2007. Cellular senescence and cancer treatment. *Biochim. Biophys. Acta.* 1775:5–20.

Solomon, J.M., R. Pasupuleti, L. Xu, T. McDonagh, R. Curtis, P.S. DiStefano, and L.J. Huber. 2006. Inhibition of SIRT1 catalytic activity increases p53 acetylation but does not alter cell survival following DNA damage. *Mol. Cell. Biol.* 26:28–38. doi:10.1128/MCB.26.1.28-38.2006

Sun, F., H. Fu, Q. Liu, Y. Tie, J. Zhu, R. Xing, Z. Sun, and X. Zheng. 2008. Downregulation of CCND1 and CDK6 by miR-34a induces cell cycle arrest. *FEBS Lett.* 582:1564–1568. doi:10.1016/j.febslet.2008.03.057

Tahara, H., M. Kusunoki, Y. Yamanaka, S. Matsumura, and T. Ide. 2005. G-tail telomere HPA: simple measurement of human single-stranded telomeric overhangs. *Nat. Methods.* 2:829–831. doi:10.1038/nmeth797

Takakura, S., N. Mitsutake, M. Nakashima, H. Namba, V.A. Saenko, T.I. Rogounovitch, Y. Nakazawa, T. Hayashi, A. Ohtsuru, and S. Yamashita. 2008. Oncogenic role of miR-17-92 cluster in anaplastic thyroid cancer cells. *Cancer Sci.* 99:1147–1154. doi:10.1111/j.1349-7006.2008.00800.x

Takeshita, F., L. Patrawala, M. Osaki, R.U. Takahashi, Y. Yamamoto, N. Kosaka, M. Kawamata, K. Kelnar, A.G. Bader, D. Brown, and T. Ochiya. 2010. Systemic delivery of synthetic microRNA-16 inhibits the growth of metastatic prostate tumors via downregulation of multiple cell-cycle genes. *Mol. Ther.* 18:181–187. doi:10.1038/mt.2009.207

Tapias, A., C.J. Ciudad, I.B. Roninson, and V. Noé. 2008. Regulation of Sp1 by cell cycle related proteins. *Cell Cycle.* 7:2856–2867. doi:10.4161/cc.7.18.6671

Tazawa, H., N. Tsuchiya, M. Izumiya, and H. Nakagama. 2007. Tumor-suppressive miR-34a induces senescence-like growth arrest through modulation of the E2F pathway in human colon cancer cells. *Proc. Natl. Acad. Sci. USA.* 104:15472–15477. doi:10.1073/pnas.0707351104

Ting, Y., D.J. Medina, R.K. Strair, and D.G. Schaar. 2010. Differentiation-associated miR-22 represses Max expression and inhibits cell cycle progression. *Biochem. Biophys. Res. Commun.* 394:606–611. doi:10.1016/j.bbrc.2010.03.030

Tryndyak, V.P., S.A. Ross, F.A. Beland, and I.P. Pogribny. 2009. Down-regulation of the microRNAs miR-34a, miR-127, and miR-200b in rat liver during hepatocarcinogenesis induced by a methyl-deficient diet. *Mol. Carcinog.* 48:479–487. doi:10.1002/mc.20484

Visone, R., P. Pallante, A. Vecchione, R. Cirombella, M. Ferracin, A. Ferraro, S. Volinia, S. Coluzzi, V. Leone, E. Borbone, et al. 2007. Specific microRNAs are downregulated in human thyroid anaplastic carcinomas. *Oncogene.* 26:7590–7595. doi:10.1038/sj.onc.1210564

Wang, G., W. Mao, S. Zheng, and J. Ye. 2009. Epidermal growth factor receptor-regulated miR-125a-5p—a metastatic inhibitor of lung cancer. *FEBS J.* 276:5571–5578. doi:10.1111/j.1742-4658.2009.07238.x

Xiong, J., Q. Du, and Z. Liang. 2010. Tumor-suppressive microRNA-22 inhibits the transcription of E-box-containing c-Myc target genes by silencing c-Myc binding protein. *Oncogene.* 29:4980–4988. doi:10.1038/onc.2010.241

DNA Repair 10 (2011) 314–321

Contents lists available at ScienceDirect

DNA Repair

journal homepage: www.elsevier.com/locate/dnarepair

Two unrelated patients with *MRE11A* mutations and Nijmegen breakage syndrome-like severe microcephaly

Yoshiyuki Matsumoto[a], Tatsuo Miyamoto[a], Hiromi Sakamoto[a], Hideki Izumi[a], Yuka Nakazawa[b], Tomoo Ogi[b], Hidetoshi Tahara[c], Shozo Oku[d], Azuma Hiramoto[e], Toshihide Shiiki[f], Yoshiki Fujisawa[g], Hirofumi Ohashi[h], Yoshihiro Sakemi[i], Shinya Matsuura[a,*]

[a] *Department of Genetics and Cell Biology, Research Institute for Radiation Biology and Medicine, Hiroshima University, Kasumi 1-2-3, Minami-ku, Hiroshima 734-8553, Japan*
[b] *Department of Molecular Medicine, Atomic Bomb Disease Institute, Nagasaki University, Sakamoto 1-12-4, Nagasaki 852-8523, Japan*
[c] *Department of Cellular and Molecular Biology, Graduate School of Biomedical Sciences, Hiroshima University, Kasumi 1-2-3, Minami-ku, Hiroshima 734-8553, Japan*
[d] *Kagoshima Kodomo Hospital, Ijuin-cho 2-2000-669, Hioki 899-2503, Japan*
[e] *Hokkaido Ryoikuen, Shunkoudai 4-10, Asahikawa 071-8144, Japan*
[f] *Tobu Ryoiku Center, Shinsuna 3-3-25, Koutou-ku 136-0075, Tokyo, Japan*
[g] *Ehime Prefectural Central Hospital, Kasugamachi 83, Matsuyama 790-0024, Japan*
[h] *Saitama Children's Medical Center, Iwatsuki-ku, Saitama 339-8551, Japan*
[i] *Beppu Medical Center, Uchikamado, Beppu 874-0011, Japan*

ARTICLE INFO

Article history:
Received 19 August 2010
Received in revised form
25 November 2010
Accepted 10 December 2010
Available online 12 January 2011

Keywords:
Nijmegen breakage syndrome (NBS)
Ataxia–telangiectasia-like disorder (ATLD)
Nijmegen breakage syndrome-like disorder (NBSLD)
ATM
MRE11
NBS1
Microcephaly

ABSTRACT

MRE11 and NBS1 function together as components of a MRE11/RAD50/NBS1 protein complex, however deficiency of either protein does not result in the same clinical features. Mutations in the *NBN* gene underlie Nijmegen breakage syndrome (NBS), a chromosomal instability syndrome characterized by microcephaly, bird-like faces, growth and mental retardation, and cellular radiosensitivity. Additionally, mutations in the *MRE11A* gene are known to lead to an ataxia–telangiectasia-like disorder (ATLD), a late-onset, slowly progressive variant of ataxia–telangiectasia without microcephaly. Here we describe two unrelated patients with NBS-like severe microcephaly (head circumference −10.2 SD and −12.8 SD) and mutations in the *MRE11A* gene. Both patients were compound heterozygotes for a truncating or missense mutation and carried a translationally silent mutation. The truncating and missense mutations were assumed to be functionally debilitating. The translationally silent mutation common to both patients had an effect on splicing efficiency resulting in reduced but normal MRE11 protein. Their levels of radiation-induced activation of ATM were higher than those in ATLD cells.

1. Introduction

The development of the central nervous system is highly sensitive to DNA damaging agents and therefore several autosomal recessive disorders with defective DNA damage repair exhibit neurological abnormalities such as microcephaly and neurodegeneration [1,2].

The MRE11/RAD50/NBS1 (MRN) protein complex and the ataxia–telangiectasia mutated (ATM) protein, together play a central role in DNA double strand break repair [3]. Mutations in the *ATM* (MIM# 607585) and *MRE11A* (MIM# 600814) genes each give rise to a progressive cerebellar ataxia syndrome: *ATM* mutations to ataxia–telangiectasia (A–T [MIM# 208900]) [4], and *MRE11A* mutations to ataxia–telangiectasia-like disorder (ATLD [MIM# 604391]) [5,6]. A–T is an autosomal recessive disorder characterized by growth deficiency, progressive cerebellar ataxia, dysarthria, telangiectasia, frequent respiratory infections, and immunodeficiency. ATLD is also characterized by cerebellar ataxia, but its onset is later in life and its progression is slower than in A–T. In addition, there is no telangiectasia and immunoglobulin levels are normal.

Mutations in two different genes involved in the MRE11/RAD50/NBS1 complex are known to lead to a hereditary disorder with severe microcephaly: the *NBN* gene (MIM# 602667) to Nijmegen breakage syndrome (NBS [MIM# 251260]) [7–9], and the *RAD50* gene (MIM# 604040) to Nijmegen breakage syndrome-like disorder (NBSLD [MIM# 613078]) [10]. NBS is an autosomal recessive disorder characterized by microcephaly, growth and mental retardation, immunodeficiency, radiosensitivity, and cancer predisposition; NBSLD is a disorder with microcephaly, mental retardation, bird-like face, and short stature,

* Corresponding author. Tel.: +81 82 257 5809; fax: +81 82 256 7101.
E-mail address: shinya@hiroshima-u.ac.jp (S. Matsuura).

1568-7864/$ – see front matter © 2010 Elsevier B.V. All rights reserved.
doi:10.1016/j.dnarep.2010.12.002

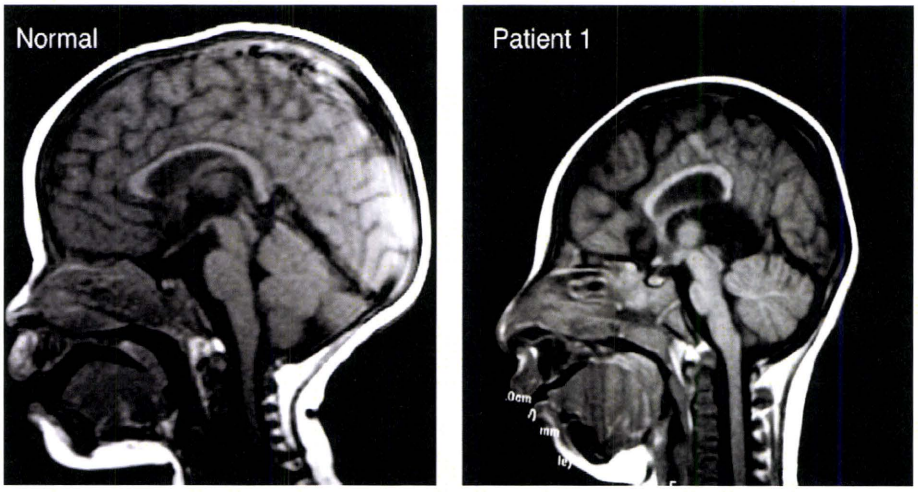

Fig. 1. Sagittal brain magnetic resonance imaging. (Left) Normal individual. (Right) Patient 1 at age 18 months with generalized cerebral hypodysplasia.

but without severe infections, immunodeficiency, or cancer predisposition.

We here describe two unrelated patients with Nijmegen breakage syndrome-like severe microcephaly and compound heterozygous mutations in the *MRE11A* gene.

2. Materials and methods

2.1. Clinical report

A 35-year-old woman was referred to us at 18 weeks of pregnancy for evaluation of intrauterine growth retardation. Ultrasound scan showed a fetus with a small femora and a disproportionately small head. Caesarian section was performed at 32 weeks of pregnancy, and a boy (Patient 1), was delivered. His birth weight was 966 g (−4.8 SD), length 35 cm (−6.7 SD), and head circumference 22 cm (−8.1 SD). He had severe microcephaly, a bird-headed facial appearance with receding forehead, and a prominent nose. Anterior fontanel was not palpable. His parents and two elder brothers were all healthy and phenotypically normal. There was no family history of consanguinity. Brain magnetic resonance imaging at age 18 months demonstrated hypoplasia of the cerebrum, smooth gyri, and enlarged lateral ventricles (Fig. 1). He had patent ductus arteriosus, which was surgically corrected at age 5 months. Bilateral cryptochidism was operated on at age 3 years. He stood holding onto a chair at age 30 months, sat alone with a stoop at age 3 years, and walked at age 3 years. At age 3.5 years, he weighed 7.4 kg (−4.1 SD), measured 78.5 cm (−4.8 SD), and had a head circumference of 34 cm (−10.2 SD). G-banded chromosomes were 46, XY. He had no severe or recurrent infections and his immunoglobulin levels were normal. Now aged 8 years, he is toilet trained, speaks several meaningful words, but does not speak a two-word-sentence. He attends a primary school, and is affable and friendly. He is farsighted with astigmatism. He is able to run with a slow pitch and kick a soccer ball. He shows neither ocular apraxia nor cerebellar ataxia.

Patient 2, a boy, was born at 37 weeks of gestation to a 29-year-old mother and a 28-year-old father, both healthy and unrelated. The pregnancy was unremarkable. An older brother was healthy without malformations. Birth weight was 1560 g (−4.1 SD), length 39 cm (−5.9 SD), and head circumference 25 cm (−6.1 SD). At age 30 months, he sat alone but could not stand or walk. At age 5 years, he shuffled while sitting, but was unable to stand. At age 13 years, he weighed 9.2 kg (−4.2 SD), measured 97 cm (−7.0 SD), and had a head circumference of 35 cm (−12.8 SD). He had severe microcephaly, a bird-like face with sloping forehead, a big nose, large and simple ears, short palpebral fissures, a small mouth, and a small and receding chin. His shoulders, elbows, hips, and knees exhibited a decreased range of motion. Also noted were scoliosis, subluxation of the left elbow joint, bilateral cryptorchidism, and bilateral talipes equinus. His tendon reflexes were slightly exaggerated. G-banded chromosomes were 46, XY. His immunoglobulin levels were normal. Now aged 33, he lives in an institution for handicapped individuals. He does not speak meaningful words, but recognizes people, communicates by gesture, and shows fondness by touching. He is bedridden, is unable to roll over, and is handfed. He did not develop secondary sexual characteristics. He does not show ocular apraxia and had neither malignancy nor severe infections.

2.2. Immortalized skin fibroblast cells

Informed consent was obtained from Patients 1 and 2 and their families prior to this study. Primary skin fibroblast cells cultured from the two patients were immortalized by transfection with an SV40 virus and phTERT retrovirus vector [11]. We used as references immortalized fibroblast cell lines (designated as SVT) from various related disorders: NBS (GM7166VA7) [12], A–T (AT5BIVA) [13], and ATLD (D6807-SVT) [6,14]. A fibroblast cell line from a normal individual (SM-SVT) served as a control. A mouse hybrid cell line A9(neo11)-1 containing human chromosome 11 was provided by Dr. M. Oshimura, and microcell-mediated chromosome transfer was performed as previously described [12]. Fibroblast cell lines were maintained in D-MEM supplemented with 10% fetal bovine serum (Hyclone, Logan, UT, USA).

2.3. EB virus-transformed lymphoblastoid cell lines (LCLs)

LCLs were established from peripheral blood lymphocytes of the two patients and their family members. We used LCLs from NBS (94P247) [9], ATLD (200704L), and A–T as references, and a LCL from a normal individual (96-007M) as a control. A NBS cell line (94P247) was provided by Dr. K. Sperling. An ATLD cell line (200704L) was established from a blood sample from a boy with ATLD [15], supplied by Drs. S. Nonoyama and K. Imai. LCLs were cultured in RPMI 1640 with 20% fetal bovine serum.

2.4. Mutational analysis

PCR primers for *MRE11A* gene (GenBank NM_005591.3) were synthesized to amplify all coding exons and intron–exon boundaries [16]. PCR products were directly sequenced using an ABI

PRISM 3130 Genetic Analyzer (Applied Biosystems, Foster City, CA). RT-PCR primers were synthesized to amplify the *MRE11A* cDNA spanning exons 1–8 (5′-CGAAAAGAAGACAGCCTTGG-3′ and 5′-TCCAAAAATTGTTCTGGAATGA-3′) (GenBank NM_005590.3). RT-PCR products were visualized following electrophoresis on a 2% NuSieve agarose gel. PCR primers for *RAD50* (GenBank Z75311.1) and *NBN* cDNAs (GenBank AF058696.2) were synthesized to amplify the open reading frame with several overlapping segments.

Transcript levels of the *MRE11A*-c.338A and *MRE11A*-c.338G alleles in LCLs from a normal individual, Patient 2 and the parents were determined by the cycleave quantitative real time PCR assay (Cycleave-qPCR, TaKaRa Co. Ltd.) carried out in triplicate. Transcripts from the *HPRT1* allele were used as a quantification control. RNaseH sensitive fluorescent probes that specifically recognize the *MRE11A*-c.338A and *MRE11A*-c.338G alleles were used for the assay. The qPCR results were analyzed by the ΔΔCT method. qPCR primers and probes used for the assay are listed below.

MRE11A-F: 5′-ACGTTTGTAACACTCGATGAA-3′;
MRE11A-R: 5′-CTGGAATTGAAATGTTGAGG-3′;
MRE11Ac.338A: (Eclipse) 5′-dAdAdG(A)dTdGdGdCdAdA-3′ (FAM);
MRE11Ac.338G: (Eclipse) 5′-dAdAdG(G)dTdGdGdCdA-3′ (ROX);
HPRT1-F: 5′-CAGGCAGTATAATCCAAAGATG-3′;
HPRT1-R: 5′-ACTGGCGATGTCAATAGGA-3′;
HPRT1-probe: (Eclipse) 5′-dCdAdGdCdA(A)dGdCdT-3′ (FAM).

2.5. Western blot analysis

Western blotting was performed as described previously [17]. Primary antibodies used were: mouse anti-MRE11 monoclonal antibody (MRE11-12D7, 1:1000, GeneTex, Irvine, CA); mouse anti-RAD50 monoclonal antibody (13B3/2C6, 1:1000, GeneTex, Irvine, CA); rabbit anti-NBS1 polyclonal antibody (NB100-142, 1:500, Novus Biologicals, Littleton, CO); mouse anti-GAPDH monoclonal antibody (6C5, 1:1000, Santa Cruz Biotechnology, Santa Cruz, CA); and mouse anti-β-tubulin monoclonal antibody (1:2000, Sigma–Aldrich, St. Louis, MO).

2.6. Radiation-sensitivity analysis

Clonogenic analysis was performed on fibroblast cell lines to learn of their radiosensitivity as previously described [12]. Chromosome breakage analysis of LCLs was carried out as follows. Cells were irradiated with 2 Gy X-ray and harvested 24 h after irradiation. Giemsa-stained chromosome slides were prepared, and chromatid or chromosome breaks and quadriradials were counted.

2.7. ATM autophosphorylation after γ-irradiation

Immortalized fibroblast cells or LCLs were irradiated with 0.5 Gy of γ ray. At 15 min and 30 min after irradiation, the cells were analyzed with Western blotting using rabbit anti-ATM-p1981 monoclonal antibody (1:1000, Epitomics Inc., Burlingame, CA) and mouse anti-ATM monoclonal antibody (2C1, 1:1000, GeneTex, Irvine, CA). Band intensities were estimated using a densitometer and are presented as means ± standard deviation. The statistical differences were analyzed with Student's *t*-test. Statistical significance was assumed for $p < 0.05$.

2.8. DNA damage response assay

ATM-dependent G2/M checkpoint arrest was performed according to the methods described previously [18].

2.9. p53 phosphorylation after γ-irradiation

Lymphoblastoid cells were irradiated with 0.5 Gy of γ ray. At 15 min and 30 min after irradiation, the cells were analyzed with Western blotting using rabbit anti-phosphorylated p53 (Ser15) polyclonal antibody (1:1000, Cell Signaling Technology, Beverly, MA) and mouse anti-p53 monoclonal antibody (1:1000, Oncogene Research Products, CA).

2.10. Caspase 3 activation after γ-irradiation

Immortalized fibroblast cells were irradiated with 0 or 10 Gy of γ ray. At 72 h after irradiation the cells were analyzed with Western blotting using rabbit anti-cleaved caspase 3 monoclonal antibody (#9664, 1:1000, Cell Signaling Technology, Beverly, MA).

3. Results

3.1. Identification of MRE11A mutations

Several studies have demonstrated that microcephaly, as was present in the two patients we described, is a common feature in a variety of DNA damage repair defective disorders [2]. Therefore, we examined DNA damage repair proteins including ATM, ATR, MRE11, RAD50, and NBS1 in the two patients. Western blot analysis showed normal levels of ATM and ATR (data not shown) and reduced levels of MRE11, RAD50, and NBS1 in both patients (Fig. 2a). We, therefore, sequenced all the *MRE11A*, *RAD50*, and *NBN* coding sequences in both patients and found only the *MRE11A* mutations c.658A>C and c.659+1G>A in Patient 1, and c.658A>C and c.338A>G in Patient 2 (Fig. 2b). In Patient 1, c.658A>C was derived from the father, and c.659+1G>A from the mother. Two brothers were a heterozygote for c.659+1G>A. RT-PCR and sequencing analysis demonstrated that c.659+1G>A resulted in exon 7 skipping leading to a premature termination codon (p.Ser183ValfsX31) (Fig. 2c). The c.658A>C substitution located within exon 7 did not alter amino acids but affected splicing efficiency that resulted in exon 7 skipping (Fig. 2c). RT-PCR analysis of exons 1–8 of *MRE11A* cDNA from Patient 1 detected a reduced but considerable amount of correctly spliced transcripts in addition to the exon-skipped transcript (Fig. 2c). Western blot analysis of fibroblasts from Patient 1 detected a reduced amount of normal-sized MRE11 protein (Fig. 2a). No smaller-sized protein corresponding to the predicted truncated form was detected in both lymphocytes and fibroblasts. The c.658A>C substitution was not found in 100 normal Japanese individuals. These results indicated that the c.658A>C mutation leads to exon 7 skipping but that some of the RNA is correctly spliced.

Patient 2 was another compound heterozygote with c.658A>C, the same single-base substitution as the one found in Patient 1, and c.338A>G, a single-base substitution in exon 5. The c.658A>C substitution was inherited from the mother while c.338A>G was derived from the father. A DNA sample from the older brother was not available. Cloning and sequencing of the RT-PCR products of Patient 2 revealed two kinds of mRNA from the c.338G allele; normal sized transcripts carrying the c.338A>G substitution and intermediately sized transcripts resulting from exon 5 skipping (Fig. 2c). The normal sized products lead to an amino acid substitution of Asp to Gly at the 113th residue (p.Asp113Gly). The 113th residue is located within the highly conserved phosphoesterase domain, which is essential for endonuclease activity [19]. On the other hand, the intermediately sized transcripts resulting from exon 5 skipping lead to a premature termination codon (p.Phe106GlnfsX10). We then examined the levels of the transcripts from the c.338A and c.338G alleles by quantitative RT-PCR analysis. The correctly spliced

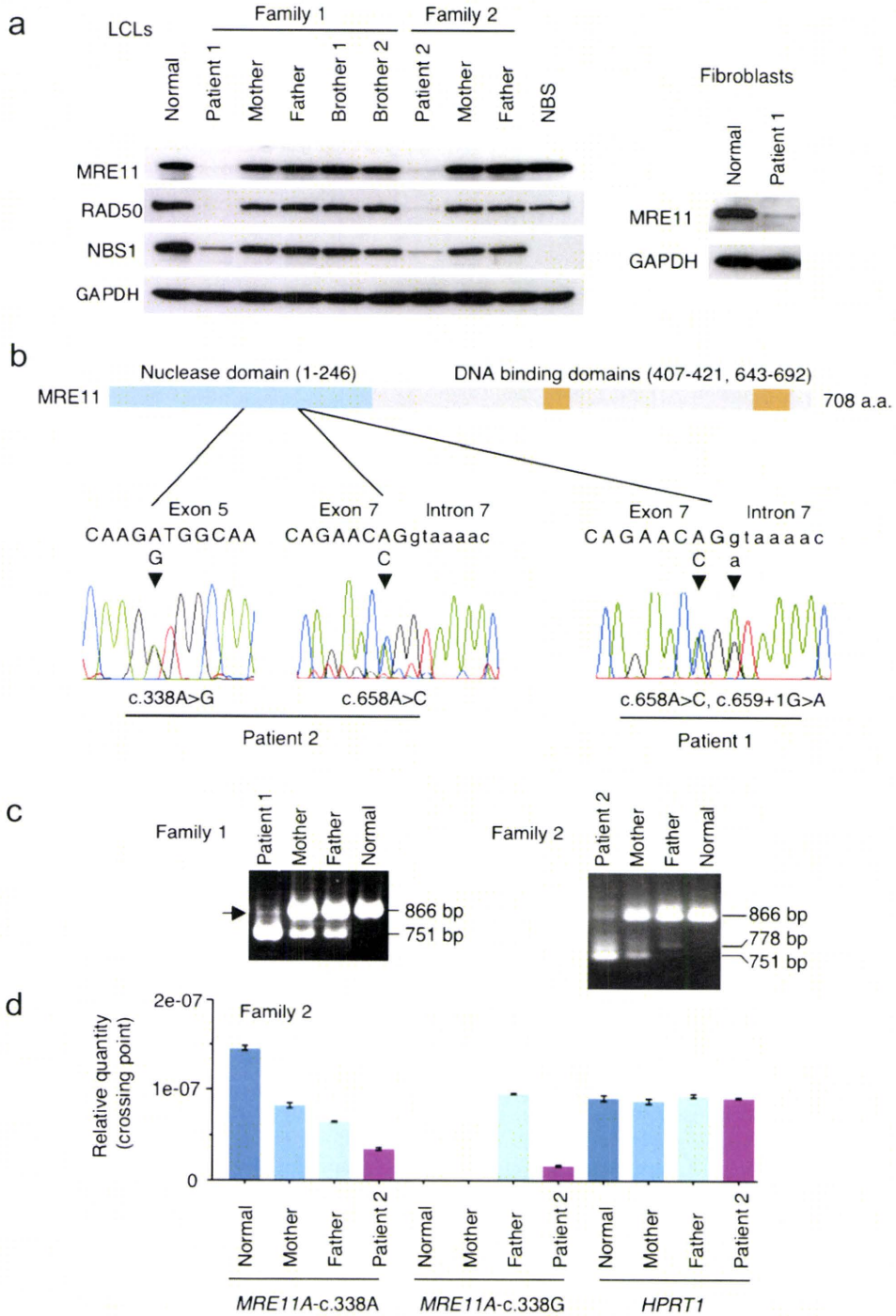

Fig. 2. MRE11 deficiencies associated with *MRE11A* mutations. (a) Western blot analyses of MRE11, RAD50, and NBS1 in lymphoblastoid cell lines (LCLs) from Patients 1 and 2 and their family members. Nijmegen breakage syndrome (NBS) cells were used as an NBS1-deficient reference, and anti-GAPDH antibody for equal loading. Levels of MRE11, RAD50, and NBS1 were reduced in both patients. Right panel shows a reduced MRE11 protein band of normal size in fibroblasts from Patient 1. (b) MRE11 protein structure and *MRE11A* mutations in Patients 1 and 2 as determined by genomic DNA sequencing. Patient 1 was a compound heterozygote with c.658A>C, a single-base substitution in exon 7, and c.659+1G>A, a substitution at an exon–intron junction of the splice donor-site. Patient 2 was a compound heterozygote with c.658A>C, the same single-base substitution in exon 7, and c.338A>G, a single-base substitution in exon 5. (c) RT-PCR analyses of exons 1–8 of *MRE11A* cDNAs from Patients 1 and 2 and their family members. RT-PCR of Patient 1 yielded two bands of 866 bp and 751 bp. The 866 bp band corresponds to the correctly spliced transcripts, and the 751 bp band to exon 7-skipped transcripts. The arrow on the left margin indicates the transcripts from the c.658A>C mutant allele. Analyses in the parents yielded two bands of 866 bp and 751 bp. RT-PCR of Patient 2 showed three bands of 866 bp, 778 bp, and 751 bp. The 866 bp band corresponds to the correctly spliced transcripts from the c.658A>C allele and the c.338A>G allele. The 778 bp band corresponds to exon 5-skipped transcripts, and the 751 bp band to the exon 7-skipped transcripts. (d) Quantitative RT-PCR analysis of the transcript levels from the c.338A and the c.338G alleles of Patient 2 and their family members. Transcripts from the *HPRT1* allele were used as a quantification control. The correctly spliced transcripts from the c.338G allele of Patient 2 showed 25% of the normal level. By contrast, the transcript levels from the c.338G allele of the father were not affected.

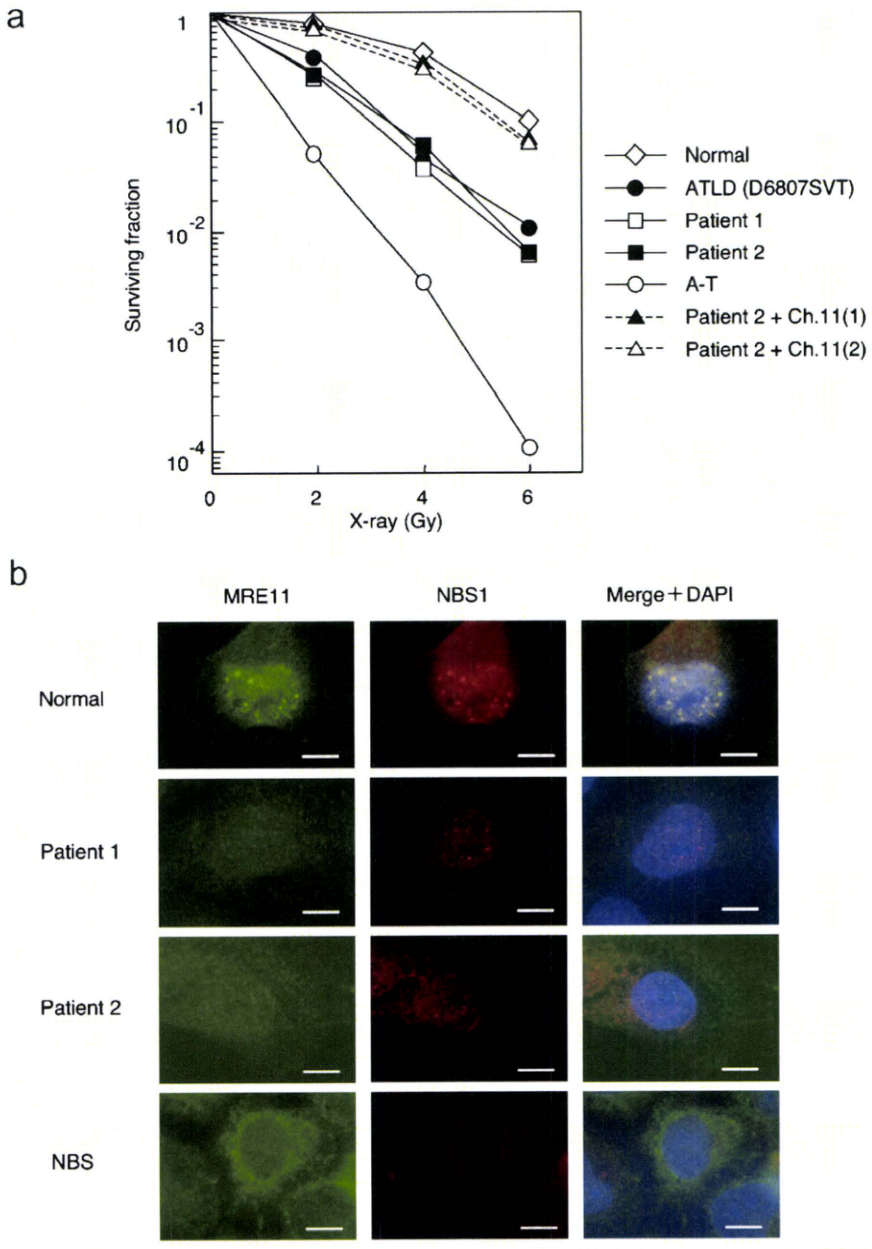

Fig. 3. Clonogenic survival curves for X-ray-irradiated fibroblasts. (a) Radiosensitivity was measured by counting colonies surviving radiation doses of 0–6 Gy. Colony survival was expressed as a logarithm. ATLD, ataxia–telangiectasia-like disorder; A–T, ataxia–telangiectasia. A–T cells were highly sensitive to radiation. Cells from Patients 1 and 2, and ATLD all showed intermediate levels of sensitivity. Microcell-mediated transfer of a human chromosome 11 (including the *MRE11A* locus) into the cells from Patient 2 restored radiation sensitivity. (b) Formation of MRE11 and NBS1 radiation-induced nuclear foci. Cells were analyzed by immuno-staining at 24 h after 6 Gy irradiation. Normal cells served as a control, and NBS cells served as an *NBN*-deficient reference. MRE11 and NBS1 formed nuclear foci after irradiation in normal cells. In contrast, cells from Patients 1 and 2 showed only very faint signals.

transcripts from the c.338G allele of Patient 2 showed 25% of the normal level (Fig. 2d). By contrast, the transcript levels from the c.338G allele of the father were not affected. The c.338A>G substitution was not detected in 100 normal Japanese individuals.

3.2. Cells from Patients 1 and 2 exhibit radiation-hypersensitivity

A clonogenic radiation sensitivity assay was performed on fibroblast cells from Patients 1 and 2 on ATLD and A–T cells as references, and on normal cells as a control. The cells from Patients 1 and 2, and ATLD were hypersensitive to X-ray irradiation, as measured by the share of surviving fractions after irradiation (Fig. 3a). A–T cells showed more marked radiation-hypersensitivity than in Patients 1 and 2, and ATLD. We introduced chromosome 11 (containing the *MRE11A* locus) into the cells from Patient 2 through microcell-mediated transfer [12]. Two microcell-hybrid clones obtained and both showed restoration of radiation-sensitivity (Fig. 3a).

Next, we studied MRE11 and NBS1 radiation-induced nuclear foci formation 24 h after exposure to 6 Gy. MRE11 and NBS1 formed nuclear foci after irradiation in normal cells. In contrast, cells from Patients 1 and 2 showed only very faint signals of NBS1 and MRE11. It is noteworthy that a few NBS1 foci were present in Patient 1. These findings are likely to be compatible with the level of the protein in the cells (Fig. 3b).

Table 1
Chromosomal aberrations in lymphocytes after 2 Gy irradiation.

Cells	No. of cells analyzed	Chromosome aberrations			Total no. of aberrations	Chromosome aberrations per cell
		Chromatid break	Chromosome break	Quadriradial chromosome		
Normal	100	10	17	3	20	0.20
ATLD	100	12	46	64	122	1.22
Patient 1	105	20	64	47	178	1.70
Patient 2	100	66	65	67	198	1.98
A–T	100	62	102	34	198	1.98

Table 1 lists chromosomal aberrations induced by ionizing radiation in LCLs from Patients 1 and 2, ATLD and A–T. Chromosome aberrations scored included chromatid and chromosome breaks and quadriradials. Cells from Patients 1 and 2 both showed an increase of aberrations comparable to those in ATLD and A–T cells.

3.3. Cells from Patients 1 and 2 have levels of ATM activation higher than those in ATLD cells

We analyzed cells from Patients 1 and 2, A–T, and ATLD for radiation-induced ATM activation. ATM is phosphorylated at serine residue 1981 in response to irradiation [20]. We therefore gave 0.5 Gy of γ ray radiation to LCLs from Patients 1 and 2, A–T, and ATLD, and analyzed with Western blotting the intensity of their phosphorylated ATM bands. The LCLs from Patients 1 and 2 showed an increased intensity of the phosphorylated ATM band after irradiation, while very little ATM phosphorylation was observed at 0 and 15 min after irradiation in ATLD cells (200704L), and a phosphorylated band appeared only after 30 min (Fig. 4a). The fibroblast cells of Patients 1 and 2, and ATLD (D6807SVT) showed responses similar to the LCLs (Fig. 4b).

3.4. Cells from Patients 1 and 2 have G2/M checkpoint defects, and levels of p53 and caspase 3 activation higher than those in ATLD cells

Mitotic index was examined in the cells irradiated with 2 Gy of γ ray in order to monitor the ATM-dependent G2/M checkpoint. Fibroblasts from Patients 1 and 2, and ATLD (D6807SVT) 30 min after irradiation all showed a slight decrease in mitotic index, intermediate between control and A–T cells. At 2 h after irradiation, cells from Patients 1 and 2 showed a decrease of mitotic index to the level of normal cells, while ATLD cells showed a response intermediate between the control and A–T cells (Fig. 5a).

We studied phosphorylation of p53, an ATM substrate, in the LCLs from Patients 1 and 2, A–T, and ATLD. The LCLs from Patients 1 and 2 showed an increase of p53 phosphorylation at serine residue 15 after irradiation, whereas ATLD cells showed a noticeably small increase of p53 phosphorylation (Fig. 5b). We also studied caspase 3 activation in the cells from Patients 1 and 2, A–T, and ATLD as an endpoint of ATM-dependent apoptosis by Western blotting. Caspase 3 cleavage was apparent after irradiation in normal cells and Patients 1 and 2 cells, but not in A–T and ATLD cells (Fig. 5c).

4. Discussion

We have described two unrelated patients with severe microcephaly resembling Nijmegen breakage syndrome (NBS). NBS is a hereditary disorder caused by biallelic mutations of the *NBN* gene [7–9]. It is characterized by severe microcephaly, a bird-like facial appearance, growth and mental retardation, chromosomal instability, and cellular radiosensitivity [21]. The two patients we described both had all these features, but they showed neither immunodeficiency nor cancer predisposition, as is typical of NBS. We sequenced the *NBN*, *MRE11A*, and *RAD50* coding sequences in both patients, and found only the *MRE11A* mutations. Patient 1 had c.658A>C substitution plus a splicing mutation in the *MRE11A* gene, and Patient 2 had c.658A>C substitution and c.338A>G substitution. The c.658A>C substitution common to both patients resulted in a reduced level of normally functioning MRE11 protein. On the other hand, the c.338A>G substitution in Patient 2 resulted in a reduced level of MRE11 protein with a single amino acid substitution in the highly conserved domain. Therefore, the splicing mutation in

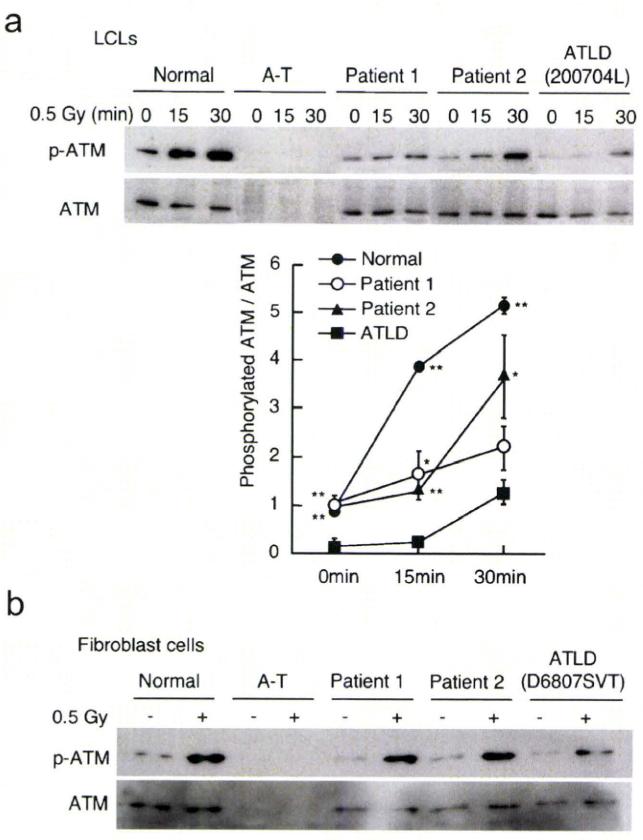

Fig. 4. Radiation-induced ATM activation. (a) Western blot analysis of phosphorylated ATM protein after irradiation of LCLs with 0.5 Gy γ ray. A–T cells served as an ATM-deficient cell line, and ATLD LCL (200704L) was used as a control. Phosphorylated ATM in LCLs from both Patients 1 and 2 increased after irradiation, while ATLD cells did not. ATLD LCL (200704L) was derived from a compound heterozygote for a *MRE11A* missense mutation (p.Trp243Arg) and a splicing mutation that resulted in exon 10 skipping, leading to an in-frame deletion (p.340–366del27) without correctly spliced transcripts [15]. The statistical significance of the differences in phosphorylated ATM/total ATM was examined by *t*-test. $^{*}p<0.05$; $^{**}p<0.01$ (normal, Patient 1, or Patient 2 versus ATLD). The data are shown as average ± standard error determined from three separate experiments. (b) Western blots of phosphorylated ATM protein at 30 min after irradiation of fibroblasts with 0.5 Gy of γ ray. A–T cells served as an ATM-deficient cell line, and ATLD fibroblasts (D6807SVT) harboring homozygous nonsense mutations were used as a control. Phosphorylated ATM in fibroblasts from both Patients 1 and 2 increased after irradiation, whereas ATLD cells did not.

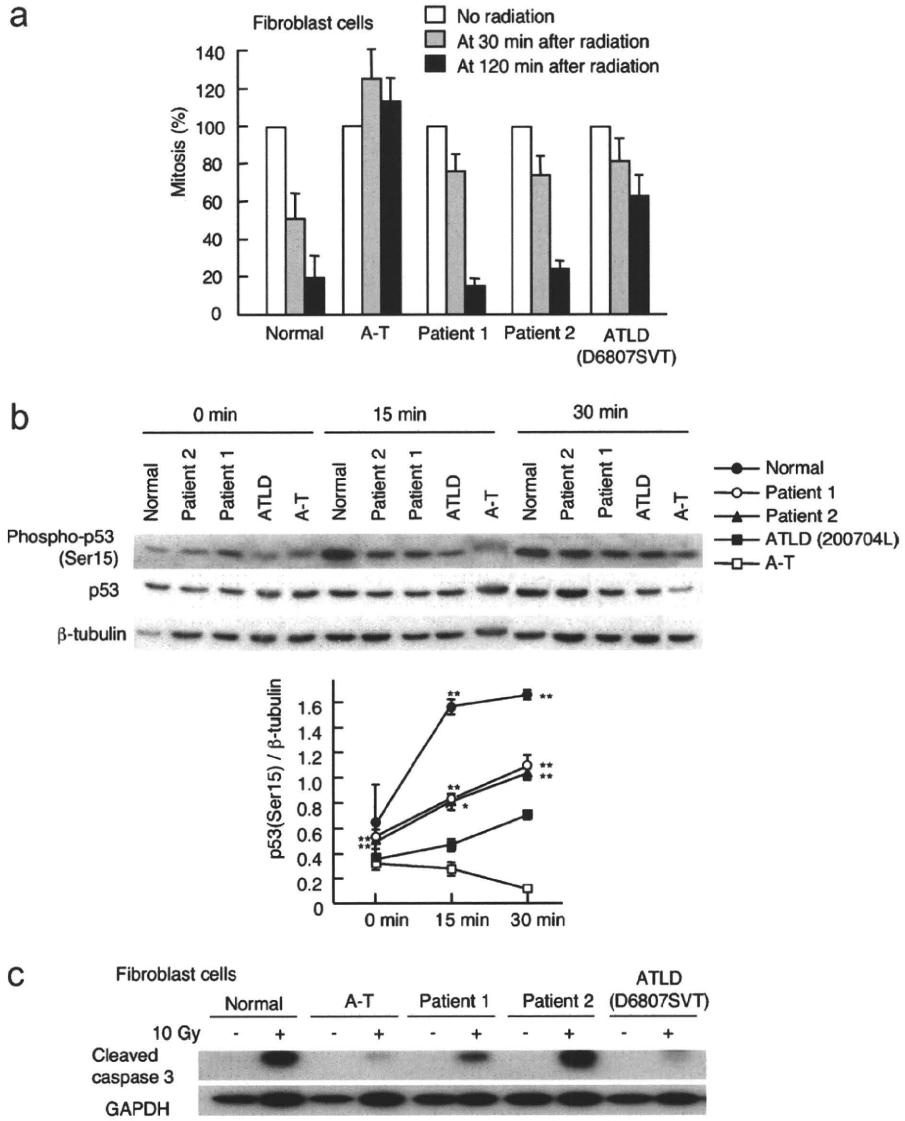

Fig. 5. Radiation-induced G2/M checkpoint and, p53 phosphorylation and caspase 3 activation as indicators of ATM activation deficiency. (a) Ataxia–telangiectasia (A–T) fibroblasts were used as an ATM-deficient reference, and ATLD fibroblasts (D6807SVT) harboring homozygous nonsense mutations were used as a control. Cultured fibroblast cells on a slide were irradiated with 2 Gy of γ ray, and stained 30 min or 2 h later with DAPI and rabbit anti-phospho-histone H3 polyclonal antibody. Mitotic index in each cell line without irradiation was estimated as 100%. Fibroblasts from Patients 1 and 2, and ATLD cells all showed a slight decrease in mitotic index at 30 min after irradiation, intermediate between normal and A–T cells. At 2 h after irradiation, cells from Patients 1 and 2 showed a decrease of mitotic index to the level of the normal cells, while ATLD cells showed a response intermediate between normal and A–T cells. Each column represents an average ± standard error from three separate experiments. (b) Western blots of phospohrylated p53 protein after irradiation. A–T and ATLD cells were used as controls. LCLs were irradiated with 0.5 Gy of γ ray. At 15 min and 30 min after irradiation, the cells were analyzed with Western blotting using rabbit anti-phosphorylated p53 (Ser15) polyclonal antibody (1:1000, Cell Signaling Technology, Beverly, MA) and mouse anti-p53 monoclonal antibody (1:1000, Oncogene Research Products, CA). Phosphorylated p53 in LCLs from Patients 1 and 2 increased after irradiation, whereas such an increase was smaller in ATLD cells. The statistical significance of the differences in phosphorylated p53/β-tubulin was tested by *t*-test. $^{*}p < 0.05$; $^{**}p < 0.01$ (normal, Patient 1, or Patient 2 versus ATLD). The data are shown as average ± standard error determined from three separate experiments. (c) Western blot analysis of cleaved caspase 3 protein after 10 Gy γ-irradiation of fibroblast cells. Cleaved caspase 3 bands were seen in normal, Patients 1 and 2 cells, but not in A–T and ATLD cells.

Patient 1 and the missense mutation in Patient 2 were assumed to be functionally debilitating.

MRE11A is known as the gene underlying ataxia–telangiectasia-like disorder (ATLD), a milder and slowly progressive variant of A–T without microcephaly [5]. To date, seven families with ATLD patients have been reported: two in the U.K., one in Italy, three in Saudi Arabia, and one in Japan. These patients with *MRE11A* mutations included: compound heterozygotes with a splicing mutation plus a missense mutation; homozygotes for a missense mutation; compound heterozygotes with a missense mutation plus a nonsense mutation; and homozygotes for a nonsense mutation.

It was reported that the MRE11/RAD50/NBS1 protein complex is involved in radiation-induced ATM activation [14]. We therefore analyzed level of radiation-induced ATM activation in cells from Patients 1 and 2, and those from ATLD patients. Cells from Patients 1 and 2 showed the level of ATM activation higher than those in ATLD cells. The cells from Patients 1 and 2 both showed the levels of p53 phosphorylation and caspase-3 activation higher than those in ATLD cells. The differences are likely to be attributable to the presence of normally functioning MRE11 protein in Patients 1 and 2.

Several explanations are conceivable for the unusual clinical features in the two patients. First, ATM-dependent neuronal apop-

tosis has been proposed as a mechanism underlying microcephaly in DNA damage disorders [2,22–24]. According to this model, the two patients might have undergone extensive neuronal apoptosis during development due to the relatively higher level of ATM activation, and developed severe microcephaly, while ATLD patients cannot activate ATM, thereby failing to engage in apoptosis but presenting with neurodegeneration. The second possibility is that the effect of microcephaly might be mediated through NBS1. Since *MRE11A* mutations often affect the levels of NBS1 and RAD50, and NBS1 deficiency uniformly leads to microcephaly, the effect of these *MRE11A* mutations might be indirect and those that result in greater diminution in the levels of NBS1 might be more prone to microcephaly. The third possibility is that an additional gene(s) other than *MRE11A* might be involved in development of microcephaly. The molecular mechanism underlying neuropathology remains to be elucidated.

In conclusion, we have identified and characterized the two patients with *MRE11A* mutations but severe microcephaly. This report suggests that MRE11 deficiency has a wider spectrum of the clinical features than that has been thought.

Conflict of interest statement

There is no conflict of interest.

Acknowledgements

We thank the families for their cooperation in the study, Drs. S. Nonoyama and K. Imai for providing ATLD cells, Dr. K. Sperling for NBS cells, Dr. M. Oshimura for a mouse hybrid cell line, Drs. J. Kobayashi and T. Ishii for discussion, Dr. M. Kobayashi for providing clinical information, and Ms. Y. Tonouchi for assistance. We thank Dr. T. Kajii for critically reading the manuscript. This work was supported by Grants-in-Aid for Scientific Research from the Ministry of Education, Culture, Sports, Science and Technology.

References

[1] A. Kulkarni, D.M. Wilson 3rd, The involvement of DNA-damage and -repair defects in neurological dysfunction, Am. J. Hum. Genet. 82 (2008) 539–566.
[2] M. O'Driscoll, P.A. Jeggo, The role of the DNA damage response pathways in brain development and microcephaly: insight from human disorders, DNA Repair (Amst.) 7 (2008) 1039–1050.
[3] M.F. Lavin, ATM and the Mre11 complex combine to recognize and signal DNA double-strand breaks, Oncogene 26 (2007) 7749–7758.
[4] M.F. Lavin, Ataxia–telangiectasia: from a rare disorder to a paradigm for cell signalling and cancer, Nat. Rev. Mol. Cell Biol. 9 (2008) 759–769.
[5] A.M. Taylor, A. Groom, P.J. Byrd, Ataxia–telangiectasia-like disorder (ATLD) – its clinical presentation and molecular basis, DNA Repair (Amst.) 3 (2004) 1219–1225.
[6] G.S. Stewart, R.S. Maser, T. Stankovic, D.A. Bressan, M.I. Kaplan, N.G. Jaspers, A. Raams, P.J. Byrd, J.H. Petrini, A.M. Taylor, The DNA double-strand break repair gene hMRE11 is mutated in individuals with an ataxia–telangiectasia-like disorder, Cell 99 (1999) 577–587.
[7] S. Matsuura, H. Tauchi, A. Nakamura, N. Kondo, S. Sakamoto, S. Endo, D. Smeets, B. Solder, B.H. Belohradsky, V.M. Der Kaloustian, M. Oshimura, M. Isomura, Y. Nakamura, K. Komatsu, Positional cloning of the gene for Nijmegen breakage syndrome, Nat. Genet. 19 (1998) 179–181.
[8] J.P. Carney, R.S. Maser, H. Olivares, E.M. Davis, M. Le Beau, J.R. Yates 3rd, L. Hays, W.F. Morgan, J.H. Petrini, The hMre11/hRad50 protein complex and Nijmegen breakage syndrome: linkage of double-strand break repair to the cellular DNA damage response, Cell 93 (1998) 477–486.
[9] R. Varon, C. Vissinga, M. Platzer, K.M. Cerosaletti, K.H. Chrzanowska, K. Saar, G. Beckmann, E. Seemanova, P.R. Cooper, N.J. Nowak, M. Stumm, C.M. Weemaes, R.A. Gatti, R.K. Wilson, M. Digweed, A. Rosenthal, K. Sperling, P. Concannon, A. Reis, Nibrin, a novel DNA double-strand break repair protein, is mutated in Nijmegen breakage syndrome, Cell 93 (1998) 467–476.
[10] R. Waltes, R. Kalb, M. Gatei, A.W. Kijas, M. Stumm, A. Sobeck, B. Wieland, R. Varon, Y. Lerenthal, M.F. Lavin, D. Schindler, T. Dork, Human RAD50 deficiency in a Nijmegen breakage syndrome-like disorder, Am. J. Hum. Genet. 84 (2009) 605–616.
[11] S.A. Carney, H. Tahara, C.D. Swartz, J.I. Risinger, H. He, A.B. Moore, J.K. Haseman, J.C. Barrett, D. Dixon, Immortalization of human uterine leiomyoma and myometrial cell lines after induction of telomerase activity: molecular and phenotypic characteristics, Lab. Invest. 82 (2002) 719–728.
[12] S. Matsuura, C. Weemaes, D. Smeets, H. Takami, N. Kondo, S. Sakamoto, N. Yano, A. Nakamura, H. Tauchi, S. Endo, M. Oshimura, K. Komatsu, Genetic mapping using microcell-mediated chromosome transfer suggests a locus for Nijmegen breakage syndrome at chromosome 8q21–24, Am. J. Hum. Genet. 60 (1997) 1487–1494.
[13] K. Komatsu, S. Kodama, Y. Okumura, M. Koi, M. Oshimura, Restoration of radiation resistance in ataxia telangiectasia cells by the introduction of normal human chromosome 11, Mutat. Res. 235 (1990) 59–63.
[14] T. Uziel, Y. Lerenthal, L. Moyal, Y. Andegeko, L. Mittelman, Y. Shiloh, Requirement of the MRN complex for ATM activation by DNA damage, EMBO J. 22 (2003) 5612–5621.
[15] N. Uchisaka, N. Takahashi, M. Sato, A. Kikuchi, S. Mochizuki, K. Imai, S. Nonoyama, O. Ohara, F. Watanabe, S. Mizutani, R. Hanada, T. Morio, Two brothers with ataxia–telangiectasia-like disorder with lung adenocarcinoma, J. Pediatr. 155 (2009) 435–438.
[16] S.A. Pitts, H.S. Kullar, T. Stankovic, G.S. Stewart, J.I. Last, T. Bedenham, S.J. Armstrong, M. Piane, L. Chessa, A.M. Taylor, P.J. Byrd, hMRE11: genomic structure and a null mutation identified in a transcript protected from nonsense-mediated mRNA decay, Hum. Mol. Genet. 10 (2001) 1155–1162.
[17] J. Kobayashi, H. Tauchi, S. Sakamoto, A. Nakamura, K. Morishima, S. Matsuura, T. Kobayashi, K. Tamai, K. Tanimoto, K. Komatsu, NBS1 localizes to gamma-H2AX foci through interaction with the FHA/BRCT domain, Curr. Biol. 12 (2002) 1846–1851.
[18] E. Griffith, S. Walker, C.A. Martin, P. Vagnarelli, T. Stiff, B. Vernay, N. Al Sanna, A. Saggar, B. Hamel, W.C. Earnshaw, P.A. Jeggo, A.P. Jackson, M. O'Driscoll, Mutations in pericentrin cause Seckel syndrome with defective ATR-dependent DNA damage signaling, Nat. Genet. 40 (2008) 232–236.
[19] R.S. Williams, G. Moncalian, J.S. Williams, Y. Yamada, O. Limbo, D.S. Shin, L.M. Groocock, D. Cahill, C. Hitomi, G. Guenther, D. Moiani, J.P. Carney, P. Russell, J.A. Tainer, Mre11 dimers coordinate DNA end bridging and nuclease processing in double-strand-break repair, Cell 135 (2008) 97–109.
[20] C.J. Bakkenist, M.B. Kastan, DNA damage activates ATM through intermolecular autophosphorylation and dimer dissociation, Nature 421 (2003) 499–506.
[21] S. Matsuura, J. Kobayashi, H. Tauchi, K. Komatsu, Nijmegen breakage syndrome and DNA double strand break repair by NBS1 complex, Adv. Biophys. 38 (2004) 65–80.
[22] P.O. Frappart, W.M. Tong, I. Demuth, I. Radovanovic, Z. Herceg, A. Aguzzi, M. Digweed, Z.Q. Wang, An essential function for NBS1 in the prevention of ataxia and cerebellar defects, Nat. Med. 11 (2005) 538–544.
[23] C. Barlow, K. Treuner, DNA instability in the brain: survival of the 'fittest', Nat. Med. 11 (2005) 474–475.
[24] E.R. Shull, Y. Lee, H. Nakane, T.H. Stracker, J. Zhao, H.R. Russell, J.H. Petrini, P.J. McKinnon, Differential DNA damage signaling accounts for distinct neural apoptotic responses in ATLD and NBS, Genes Dev. 23 (2009) 171–180.

THE JOURNAL OF BIOLOGICAL CHEMISTRY VOL. 285, NO. 43, pp. 33018–33027, October 22, 2010

Pin1 Associates with and Induces Translocation of CRTC2 to the Cytosol, Thereby Suppressing cAMP-responsive Element Transcriptional Activity*[S]

Received for publication, April 26, 2010, and in revised form, July 9, 2010 Published, JBC Papers in Press, July 30, 2010, DOI 10.1074/jbc.M110.137836

Yusuke Nakatsu,[a1] Hideyuki Sakoda,[b1] Akifumi Kushiyama,[c] Hiraku Ono,[b] Midori Fujishiro,[b] Nanao Horike,[d] Masayasu Yoneda,[a] Haruya Ohno,[a] Yoshihiro Tsuchiya,[a] Hideaki Kamata,[a] Hidetoshi Tahara,[e] Toshiaki Isobe,[f] Fusanori Nishimura,[g] Hideki Katagiri,[h] Yoshitomo Oka,[h] Toshiaki Fukushima,[a] Shin-Ichiro Takahashi,[i] Hiroki Kurihara,[d] Takafumi Uchida,[j] and Tomoichiro Asano[a2]

From the [a]Department of Medical Science, Graduate School of Medicine, University of Hiroshima, 1-2-3 Kasumi, Minami-ku, Hiroshima City, Hiroshima 734-8553, Japan, the Departments of [b]Internal Medicine and [d]Physiological Chemistry and Metabolism, Graduate School of Medicine, and the [i]Department of Applied Biological Chemistry, Graduate School of Agricultural and Life Sciences, University of Tokyo, 7-3-1 Hongo, Bunkyo-ku, Tokyo 113-0033, Japan, the [c]Institute for Adult Disease, Asahi Life Foundation, Tokyo 100-0006, Japan, the [e]Department of Cellular and Molecular Biology, Graduate School of Biomedical Sciences, Hiroshima University, Hiroshima 734-8553, Japan, the [f]Center for Priority Areas, Tokyo Metropolitan University, Hachioji, Tokyo 192-0397, Japan, the [g]Department of Dental Science for Health Promotion, Hiroshima University Graduate School of Biomedical Sciences, Hiroshima 734-8553, Japan, the [h]Division of Molecular Metabolism and Diabetes, Tohoku University Graduate School of Medicine, 2-1 Seiryo-machi, Aoba-ku, Sendai 980-8575, Japan, and the [j]Department of Molecular Cell Biology, Graduate School of Agricultural Science, Tohoku University, Sendai, Miyagi 981-8555, Japan

Pin1 is a unique regulator, which catalyzes the conversion of a specific phospho-Ser/Thr-Pro-containing motif in target proteins. Herein, we identified CRTC2 as a Pin1-binding protein by overexpressing Pin1 with Myc and FLAG tags in mouse livers and subsequent purification of the complex containing Pin1. The association between Pin1 and CRTC2 was observed not only in overexpression experiments but also endogenously in the mouse liver. Interestingly, Ser^{136} in the nuclear localization signal of CRTC2 was shown to be involved in the association with Pin1. Pin1 overexpression in HepG2 cells attenuated forskolin-induced nuclear localization of CRTC2 and cAMP-responsive element (CRE) transcriptional activity, whereas gene knockdown of Pin1 by siRNA enhanced both. Pin1 also associated with CRTC1, leading to their cytosol localization, essentially similar to the action of CRTC2. Furthermore, it was shown that CRTC2 associated with Pin1 did not bind to CREB. Taken together, these observations indicate the association of Pin1 with CRTC2 to decrease the nuclear CBP·CRTC·CREB complex. Indeed, adenoviral gene transfer of Pin1 into diabetic mice improved hyperglycemia in conjunction with normalizing phosphoenolpyruvate carboxykinase mRNA expression levels, which is regulated by CRE transcriptional activity. In conclusion, Pin1 regulates CRE transcriptional activity, by associating with CRTC1 or CRTC2.

Pin1 was initially cloned as a NIMA kinase-interacting protein (1). Since its discovery, numerous proteins have been identified as Pin1 substrates, including p53, cyclin D1, and Tau (2–5). Pin1 interacts with a number of target proteins through recognition of phospho-Ser/Pro motifs, and the proline conformational change induced by Pin1 modifies the structures and functions, such as stabilization, phosphorylation, and translocation, of target proteins (4–7). Pin1 possesses the WW and PPIase[3] domains in its N-terminal (amino acids 1–38) and C-terminal (amino acids 39–163) regions, respectively. To date, many reports have supported an important role for Pin1 in diseases such as cancer and Alzheimer disease (4, 5). In this study, we demonstrated that Pin1 is also involved in metabolic disease via regulation of CRTC2 (CREB-regulated transcriptional co-activator 2; also known as TORC).

The cAMP-responsive element (CRE)-binding protein (CREB) stimulates transcriptional activity through recruitment of the histone acetylase CBP and through an association with CRTC, leading to formation of the CREB·CBP·CTRC complex on a CRE site (8–16). Thus, multiple molecular mechanisms affect the CREB·CBP·CTRC complex, resulting in the regulation of CRE transcriptional activity. They include the phosphorylations of CREB at Ser^{133}, CBP at Ser^{436}, and CRTC2 at Ser^{171} (16, 17). The phosphorylation of CRTC2 at Ser^{171} reportedly leads to an association with 14-3-3 protein and thereby to its nuclear exclusion and degradation (16).

The CRTC family consists of three members, CRTC1, CRTC2, and CRTC3 (16, 18). CRTC1 is highly expressed in the brain, whereas the other two are ubiquitously expressed (19). In the liver, insulin induces the phosphorylation of CRTC2 at Ser^{171}, and this phosphorylation leads to the aforementioned

* This work was supported in part by Grant-in-aid for Young Scientists 20790648 (to Y. N.) from the Ministry of Education, Science, Sports, and Culture, Japan.
[S] The on-line version of this article (available at http://www.jbc.org) contains supplemental Figs. 1–8.
[1] These authors contributed equally to this work.
[2] To whom correspondence should be addressed. Tel.: 81-82-257-5135; Fax: 81-82-257-5136; E-mail: asano-tky@umin.ac.jp.

[3] The abbreviations used are: PPIase, peptidyl-prolyl *cis/trans*-isomerase; CRE, cAMP-response element; CREB, CRE-binding protein; NLS, nuclear localization signal; MEF, mouse embryo fibroblast; STZ, streptozotocin; PEPCK, phosphoenolpyruvate carboxykinase; CRTC, CREB-regulated transcriptional co-activator.

association with 14-3-3 protein and the nuclear exclusion and degradation of CRTC2 (16, 20). In contrast, glucagon induces dephosphorylation of CRTC2 and translocation from the cytosol to the nucleus, thereby forming the CREB·CBP·CRTC2 complex and inducing gluconeogenesis (21). Thus, CRTC2 plays important roles in hepatic glucose metabolism.

In this study, we identified CRTC2 as a Pin1-binding protein. Interestingly, the portion of CRTC2 responsible for the association with Pin1 was revealed to be in the nuclear localization signal (NLS) domain. Herein, we demonstrate that Pin1 regulates the functions and subcellular localizations of CRTC family proteins, thereby altering CRE transcriptional activity.

EXPERIMENTAL PROCEDURES

Materials—Anti-Pin1 antibody was generated by immunizing rabbits with the peptide QMQKPFEDASFATRTGEMSGPVFTDSGIHIITRTE (amino acids 129–163 of human Pin1). Anti-FLAG tag and Myc tag antibodies were purchased from Sigma-Aldrich. The antibodies against CRTC2, CREB, 14-3-3 protein, GFP, and DsRed were purchased from Cell Signaling Technology. Anti-rabbit HRP antibodies conjugated to horseradish peroxidase were obtained from Amersham Biosciences. Dulbecco's modified Eagle's medium (DMEM) and fetal bovine serum were purchased from Invitrogen. All other reagents were of analytical grade.

Preparation of Adenoviruses Expressing MEF-tagged Pin1, CRTC1, and CRTC2—The Myc-TEV-FLAG (MEF) tag cassette was generated by DNA synthesis and inserted into cloning sites in the mammalian expression vector pcDNA3 (Invitrogen; termed pcDNA3-MEF), as reported previously (22). To create the N-terminally MEF-tagged Pin1 construct, human Pin1 cDNA was inserted into pcDNA3-MEF. Then the coding portion of MEF-tagged Pin1 was isolated from pcDNA3-MEF-Pin1, and the recombinant adenoviruses containing the cDNA coding for MEF-tagged Pin1 were constructed as described previously (22). Recombinant adenoviruses expressing human Pin1 with the C-terminal HA tag or N-terminal MEF tag were also constructed and used for adenoviral gene transfer to HepG2 cells and mouse liver. Similarly, adenoviruses expressing GFP-tagged CTRC1, CRTC2, and GFP-tagged CRTC2 were prepared. Adenovirus encoding LacZ served as a control, and the adenoviral gene transfer was performed as reported previously (22).

Purification of MEF-tagged Pin1 from Mouse Livers—Recombinant adenovirus expressing MEF-tagged Pin1 was generated, purified, and concentrated using cesium chloride ultracentrifugation as reported previously (22). Adenovirus encoding LacZ served as a control. Male mice, 9 weeks of age, were obtained from the Nippon Bio-Supp. Center (Tokyo, Japan). They were injected, via the tail vein, with adenovirus at a dose of 2.5×10^7 plaque-forming units/g body weight. Four days after adenovirus injection, the mouse livers were removed and lysed in lysis buffer (50 mM Tris-HCl, pH 7.5, 150 mM NaCl, 10% (w/v) glycerol, 100 mM NaF, 10 mM EGTA, 1 mM Na_3VO_4, 1% (w/v) Triton X-100, 5 μM $ZnCl_2$, 2 mM phenylmethylsulfonyl fluoride, 10 μg/ml aprotinin, and 1 μg/ml leupeptin). The lysates were centrifuged at 100,000 × *g* for 20 min at 4 °C. The supernatant was passed through a 5-μm filter, incubated with 150 μl of Sepharose beads for 60 min at 4 °C and then passed through a 0.65-μm filter. The filtrated supernatant was mixed with 150 μl of anti-Myc-conjugated Sepharose beads for the first immunoprecipitation. After incubation for 90 min at 4 °C, the beads were washed five times with 1.5 ml of TNTG buffer (20 mM Tris-HCl, pH 7.5, 150 mM NaCl, 10% (w/v) glycerol, 0.1% (w/v) Triton X-100), twice with buffer A (20 mM Tris-HCl, pH 7.5, 150 mM NaCl, and 0.1% (w/v) Triton X-100), and finally once with TNT buffer (50 mM Tris-HCl, pH 8.0, 150 mM NaCl, 0.1% (w/v) Triton X-100). The washed beads were incubated with 15 units of TEV protease (Invitrogen) in 150 μl of TNT buffer to release bound materials from the beads. After incubation for 60 min at room temperature, the supernatant was pooled, and the beads were washed twice with 75 μl of buffer A. The resulting supernatants were combined and incubated with 25 μl of FLAG-Sepharose beads for the second immunoprecipitation. After incubation for 60 min at room temperature, the beads were washed three times with 500 μl of buffer A, and proteins bound to the FLAG beads were dissociated by incubation with 1 mM synthetic FLAG peptides in buffer A for 120 min at 4 °C. Approximately 3 μg of protein (0.01% of starting materials) were routinely recovered by this procedure. The samples were electrophoresed and subjected to SDS-PAGE and immunoblotting.

Cell Culture—Sf9 cells were grown in TC100 (Invitrogen) medium containing 10% fetal calf serum at 27 °C. HepG2 hepatoma cells were grown in DMEM containing 10% fetal calf serum at 37 °C in 5% (v/v) CO_2 in air.

Preparation of Baculoviruses Expressing Pin1 and CRTC2 Constructs—The full-length coding regions of human Pin1, GFP, GFP-tagged Pin1, CRTC2, and DsRed-tagged full-length and various deletion mutant forms of CRTC2 and S136A CRTC2 were subcloned into pBacPAK9 transfer vector (Clontech), and the baculoviruses were prepared according to the manufacturer's instructions. For protein production, Sf9 cells were infected with these baculoviruses and grown for 48 h.

Preparation of Glutathione S-Transferase (GST)-Pin1 Fusion Protein—The cDNAs encoding full-length human Pin1, the WW domain of Pin1, and the PPIase domain of Pin1 were subcloned into a pGEX-5X-1 vector (Amersham Biosciences), which was used to transform *Escherichia coli* JM105 (Promega). Transformed cells were grown to an A_{600} of 0.6 in LB medium supplemented with 0.1 mg/ml ampicillin and stimulated for 3 h with 1.0 mM isopropyl-β-D-thiogalactopyranoside. GST fusion proteins were conjugated to glutathione-Sepharose 4B (Amersham Biosciences) and used for GST pull-down experiments.

GST Pull-down—HepG2 cells expressing MEF-CTRC2 and its mutants were homogenized with homogenizing buffer (20 mmol/liter Tris/HCl (pH 7.4), 1% Triton X-100, 0.25% sodium deoxycholate, 0.25 mol/liter NaCl) containing 0.2 mmol/liter phenylmethylsulfonyl fluoride and 5 μg/ml aprotinin and centrifuged at 15,000 rpm for 30 min at 4 °C, and the supernatants were then recentrifuged at 100,000 × *g* for 1 h. The supernatants (2 μg/ml protein concentration) were incubated with 1 ml of glutathione-Sepharose 4B for 1 h at 4 °C to remove nonspecifically bound proteins and then incubated with purified GST alone, GST-Pin1, and GST-Pin1 deletion mutant proteins for 1 h and finally washed six times with homogenizing buffer. glutathione-Sepharose 4B beads

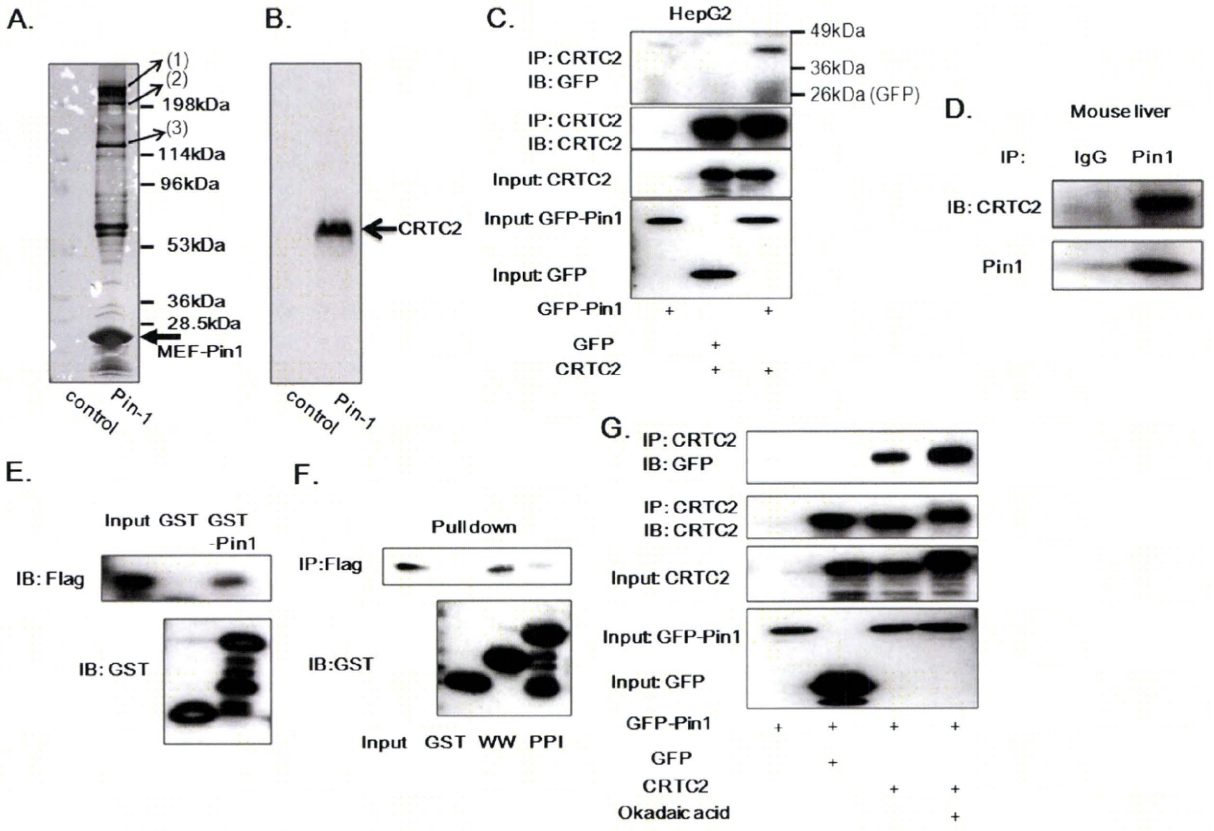

FIGURE 1. **Pin1 associates with CRTC2.** *A* and *B*, Pin1 with the N-terminal MEF tag was overexpressed in the mouse liver using adenovirus gene transfer, and the Pin1-containing complex was purified. The samples were electrophoresed and subjected to silver staining (*A*). Analysis using LC/MS revealed: *Band* (*1*), DNA-directed RNA polymerase II A; *Band* (*2*), suppressor of Ty 6 homolog + DNA-directed RNA polymerase II A; *Band* (*3*), DNA-directed RNA polymerase II polypeptide B + DNA-directed RNA polymerase I. *B*, the samples were subjected to the immunoblotting with anti-CRTC2 antibody. *C*, CRTC2 or control LacZ was overexpressed with GFP or GFP-Pin1. Then the cell lysates were immunoprecipitated (*IP*) with anti-CRTC2 antibody, followed by immunoblotting (*IB*) with anti-GFP antibody. *D*, the cell lysates from the mouse liver were immunoprecipitated with control IgG or anti-Pin1, and the immunoprecipitates were then immunoblotted with anti-CRTC2 and anti-Pin-1. *E*, HepG2 cell lysates expressing CRTC2 with a FLAG tag were incubated with glutathione beads conjugated with GST or GST-Pin1. After washing the beads, SDS-PAGE was performed followed by immunoblotting with anti-FLAG or anti-GST antibodies. *F*, HepG2 cell lysates expressing CRTC2 with a FLAG tag were incubated with glutathione beads conjugated with GST, the GST-WW domain, or the GST-PPI domain. After washing the beads, SDS-PAGE was performed, followed by immunoblotting with anti-FLAG or anti-GST antibodies. *G*, CRTC2 and either GFP or GFP-Pin1 were simultaneously overexpressed in HepG2 cells. With or without okadaic acid treatment for 0.5 h, the cell lysates were immunoprecipitated with anti-CRTC2, followed by immunoblotting with anti-GFP antibody. Representative immunoblotting data from three independent experiments are shown.

were boiled in Laemmli sample buffer, which was used for the SDS-PAGE and immunoblotting.

Preparation of Streptozotocin-treated Diabetic Mice and Gene Transfer of Pin1 into Mouse Livers—Streptozotocin (STZ)-treated diabetic male C57BL/6 mice (8–10 weeks of age) were prepared as reported previously (20). These mice were injected, via the tail vein, with adenovirus at a dose of 2.5×10^7 plaque-forming units/g body weight. Animals were fasted for 14 h and then were refed for 4 h before sacrifice. Blood glucose was measured with a portable blood glucose monitor, Glutest-Ace (Sanwa Kagaku Kenkyusho, Nagoya, Japan). All animal studies were conducted according to the Japanese guidelines for the care and use of experimental animals.

Immunoprecipitation and Immunoblotting—For the immunoprecipitation experiments, whole-cell extracts from HepG2 or Sf9 cells or mouse liver lysates obtained after an overnight fast were prepared in lysis buffer, as described above. Cell or tissue extracts were incubated for 4 h at 4 °C with the indicated antibody and then for 1 h with 30 μl of protein G-Sepharose beads. The pellets were washed five times with 1 ml of lysis buffer and then resuspended in Laemmli sample buffer, boiled for 3 min, and analyzed on SDS-polyacrylamide gels.

Western blot analysis was carried out as described previously (22). In brief, 10 μg of protein were separated by SDS-PAGE and electrophoretically transferred to polyvinylidene difluoride membranes in a transfer buffer consisting of 20 mM Tris-HCl, 150 mM glycine, and 20% methanol. The membranes were blocked with 5% nonfat dry milk in Tris-buffered saline with 0.1% Tween 20 and incubated with specific antibodies, followed by incubation with horseradish peroxidase-conjugated secondary antibodies. The antigen-antibody interactions were visualized by incubation with ECL chemiluminescence reagent (Amersham Biosciences).

Immunostaining—HepG2 cells were fixed with 4% paraformaldehyde for 10 min, rinsed with phosphate-buffered saline (PBS), and then exposed to 0.2% Triton X-100 in PBS for 5 min. Cells were subsequently incubated for 1 h at room temperature with anti-rabbit CRTC2 (1:500), and fluorescein isothiocya-

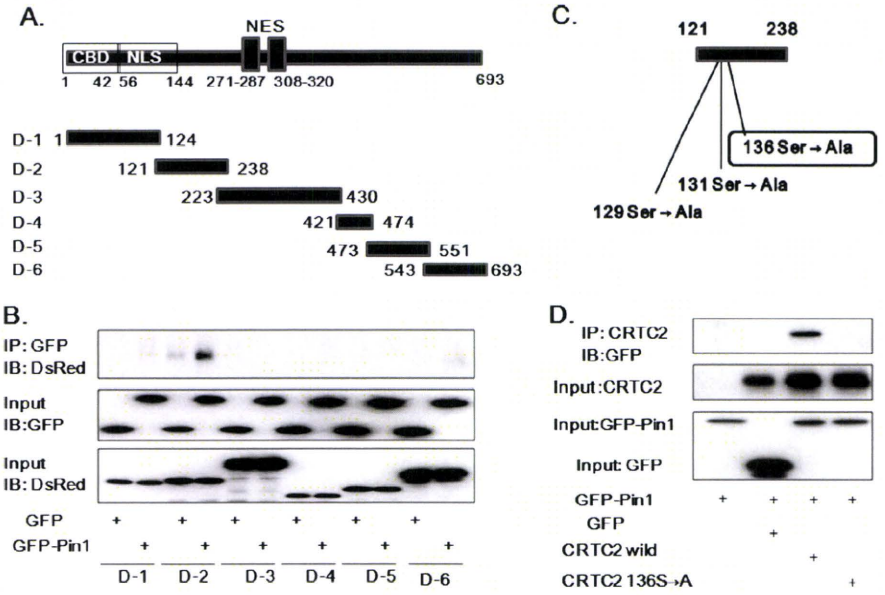

FIGURE 2. **Pin1 associates with the NLS domain of CRTC2.** *A*, the constructs of CRTC2 deletion mutants and baculoviruses expressing these six mutants with the C-terminal DsRed tag were prepared. *B*, the six deletion mutants with C-terminal DsRed tags were overexpressed with GFP or GFP-Pin1 in Sf9 cells. The cell lysates were immunoprecipitated (*IP*) with anti-GFP antibody, followed by immunoblotting (*IB*) with anti-DsRed antibody. The *upper panel* shows the binding of the Deletion-2 mutant to GFP-Pin1 but not to GFP alone. *C*, the orientations of three candidate Ser/Pro motifs in the Deletion-2 mutant involved in the association with Pin1. *D*, wild-type CRTC2 or CRTC2 S136A was overexpressed with GFP-Pin1 or GFP in Sf9 cells. The cell lysates were immunoprecipitated with anti-CRTC2 antibody followed by immunoblotting with anti-GFP. The *upper panel* shows that CRTC2 S136A does not associate with Pin1, unlike the wild-type CRTC2. Representative immunoblotting data from three independent experiments are shown.

nate-labeled anti-rabbit IgG (1:750) was used as the secondary antibody. Immunofluorescence was visualized with a laser-scanning confocal imaging system.

Luciferase Assay—The following plasmids were obtained from commercial sources: pTAL and pTAL-CRE from Clontech (Palo Alto, CA), pM from Stratagene (La Jolla, CA), and pGL4 and pRL-TK from Promega (Madison, WI). HepG2 cells in a 24-well collagen-coated plate were co-transfected with pTAL-CRE vector (0.25 μg/well) with an internal reporter, pRL-TK (0.25 μg). Luciferase activities were determined using the Dual-Luciferase Reporter Assay System (Promega Corp.).

RNA Analysis—RNA extractions were carried out using TRIzol, followed by purification over a QIAEASY RNA column. Reverse transcription and quantitative PCR were carried out as already described. The primer set for human phosphoenolpyruvate carboxykinase (PEPCK) was GGTTCCCAGGGTGCATGAAA and CACGTAGGGTGAATCCGTCAG (114 bp), and that for human GAPDH was ACCACAGTCCATGCCATCAC and TCCACCACCCTGTTGCTGTA (451 bp).

Chromatin Immunoprecipitation Assay with Anti-CRTC2, CBP, or CREB Antibodies—HepG2 cells with or without forskolin stimulation were immunoprecipitated with anti-CRTC2, anti-CBP, or anti-CREB antibody, using the Chip-IT™ express enzymatic kit (Active Motif Corp.). Then precipitated DNA was amplified by PCR using primers against the relevant promoters.

Statistical Analysis—Results are expressed as means ± S.E., and significance was assessed using one-way analysis of variance unless otherwise indicated.

RESULTS

Identification of CRTC2 in the Pin1-containing Complex from Mouse Liver—The adenovirus to MEF-tagged Pin1 was introduced into mice, and the Pin1-containing complex was purified. Purified Pin1 in the complex was electrophoresed and subjected to silver staining, which showed the presence of Pin1 bait proteins and many binding proteins (Fig. 1*A*). Bands (1), (2), and (3) were identified to be DNA-directed RNA polymerase II A, DNA-directed RNA polymerase IIB, and DNA-directed RNA polymerase I by the analysis using LC/MS, which agree with previous reports (23). Then we performed the immunoblotting using many antibodies to detect another protein included in the Pin1-containing complex because many faint bands were visible with silver staining.

Many transcriptional co-activators are included among the target proteins of Pin1 (4, 5). In addition, although one of the regulatory mechanisms of Pin1 is protein stabilization, recent reports have shown that Pin1 is involved in translocation of target proteins, such as Bax (24). These results suggest that CRTC2 is a candidate Pin1 target protein because CRTC2 is a transcriptional co-activator and is translocated between the cytosol and the nucleus. As a result, immunoblotting using anti-CRTC2 antibody indicated the presence of CTRC2 in the Pin1 complexes (Fig. 1*B*). To confirm the association between CTRC2 and Pin1, CRTC2 and each GFP-Pin1 or GFP were simultaneously overexpressed in HepG2 and Sf9 cells. As shown in Fig. 1*C* and supplemental Fig. 1, GFP-Pin1, but not GFP alone was detected in the anti-CRTC2 immunoprecipitate. Furthermore, CRTC2 was detected in the immunoprecipitate with anti-Pin1 antibody but not that with the control IgG from mouse liver (Fig. 1*D*). Thus, the association between CRTC2 and Pin1 is physiological.

Pin1 possesses the WW and PPIase domains in its N terminus (amino acids 1–38) and C terminus (amino acids 39–163), respectively. To identify the domain of Pin1 responsible for the association with CRTC2, we prepared GST-Pin1, the GST-Pin1 WW domain, and the GST-Pin1 PPIase domain. These GST proteins were conjugated to beads, followed by incubation with cell lysates from MEF-tagged CRTC2 overexpressing HepG2 cells. GST-Pin1 but not GST alone bound to CRTC2 *in vitro* (Fig. 1*E*). Using this pull-down system, it was shown that the GST-WW domain, but not the GST-PPIase domain, binds to CRTC2 (Fig. 1*F*). In addition, okadaic acid treatment significantly increased the association of CRTC2 with Pin1 (Fig. 1*G*),

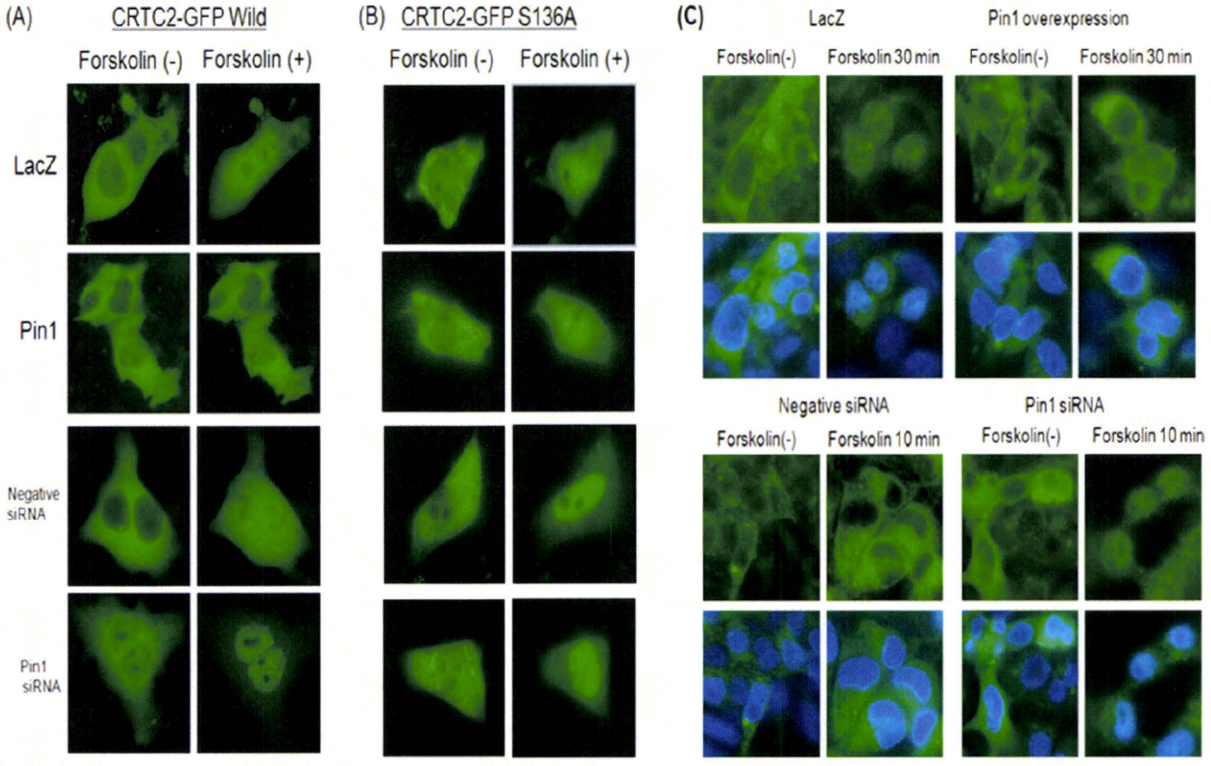

FIGURE 3. **Effect of Pin1 on subcellular localization of GFP-tagged CRTC2.** *A* and *B*, LacZ or Pin1 was overexpressed, or HepG2 cells were treated with control or Pin1 siRNAs. Then GFP-tagged CRTC2 was overexpressed in HepG2 cells. These cells were treated with forskolin, and the subcellular localization of GFP-tagged wild type or S136A CRTC2 was examined at the indicated periods after initiating forskolin stimulation. Representative data from four independent experiments are shown. *C*, LacZ or Pin1 was overexpressed in HepG2 cells, or the cells were treated with control or Pin1 siRNAs. These cells were treated with forskolin, and the subcellular localization of endogenous CRTC2 was determined by immunostaining at 10 or 30 min after initiating forskolin stimulation. Nuclei were stained with DAPI. Representative data from five independent experiments are shown.

suggesting the involvement of serine and/or threonine phosphorylation(s) in CRTC2.

Pin1 Associates with Ser^{136}-containing Motif in the NLS Domain of CRTC2—Subsequently, to reveal the domain of CRTC2 responsible for the association with Pin1, six Ds-Red-tagged CRTC2 N terminus deletion mutants (Fig. 2*A*) and GFP-tagged Pin1 were simultaneously overexpressed in Sf9 cells. As shown in Fig. 2*B*, CRTC2 deletion mutant 2 (D-2), containing amino acids 121–238, was immunoprecipitated with GFP-tagged Pin1 but not with GFP alone. This portion contains three serine-proline motifs (Fig. 2*C*). Each of these serine residues was replaced with alanine, creating a mutant that did not associate with Pin1. As shown in Fig. 2*D*, CRTC2 with serine 136 replaced by alanine did not bind to Pin1, whereas CRTC with serine 129 or 131 bound to Pin1 (data not shown). These observations indicated that the association between CRTC2 and Pin1 is mediated via the phosphoserine 136-containing motif in CRTC2 and the WW domain in Pin1. Ser^{136} is in the NLS domain, and a high level of Ser^{136} phosphorylation was demonstrated in a previous report (16).

Pin1 Inhibits CRTC2 Translocation from the Cytosol to the Nucleus—To test whether or not the effect of Pin1 on CRE transcriptional activity is mediated via the effect on the subcellular localization of CRTC2, the GFP-tagged CRTC2 was overexpressed, and the effects of the Pin1 expression level on the subcellular localization of GFP-tagged CRTC2 were analyzed in the absence or presence of forskolin stimulation (Fig. 3*A*). In the control LacZ-overexpressing or control siRNA-treated HepG2 cells, GFP-tagged CRTC2 was translocated from the cytosol to the nucleus, as reported previously (9). Pin1 overexpression markedly inhibited forskolin-induced translocation of CRTC2 into the nucleus. In addition, gene silencing of Pin1 using siRNA markedly enhanced the nuclear translocation of Pin1 in comparison with treatment with control siRNA. Although nuclear CRTC2 S136A (unable to bind to Pin1) was required for forskolin stimulation, it had no effect on either Pin1 overexpression or Pin1 siRNA (Fig. 3*B*).

In addition, we investigated the effect of Pin1 on the distribution of CRTC2 S171A. CRTC2 S171A (unable to bind to 14-3-3) was mainly present in the nucleus regardless of forskolin stimulation (supplemental Fig. 2). Pin1 overexpression slightly increased CRTC2 S171A in the cytosol, whereas Pin1 siRNA treatment reduced the amount of CRTC2 S171A in the cytosol. This effect of Pin1 was essentially in agreement with the results obtained for wild-type CRTC2.

Similar results were obtained by immunostaining the endogenous CRTC2 in HepG2 cells (Fig. 3*C*). Pin1 overexpression attenuated the forskolin-induced nuclear translocation of CRTC2 as compared with LacZ overexpression. On the other hand, treatment with Pin1 siRNA increased CRTC2 in the nucleus under forskolin stimulation as compared with the control siRNA.

Neither the distribution nor the expression of Pin1 was changed by forskolin or insulin stimulation (supplemental Fig. 3). Thus, a change in Pin1 is not required for regulation of the CRTC2 distribution.

Pin1 Associates with CRTC1 and Induces Its Localization in the Cytosol—The CRTC family consists of three isoforms, CRTC1, CRTC2, and CRTC3. The motif of CRTC2 responsible for the association with Pin1 is present in the NLS and is conserved in CRTC1 but not in CRTC3 (supplemental Fig. 4*A*). Thus, the associations of Pin1 with CRTC1 were also investigated using HepG2 cells. As shown in supplemental Fig. 4*B*, FLAG-tagged CRTC1 was detected in anti-GFP immunoprecipitates from the cells expressing GFP-tagged Pin1 and FLAG-tagged CRTC1. As shown in supplemental Fig. 4*C*, FLAG-tagged CRTC1, in which serine 155 is replaced with alanine, did not bind to GFP-tagged Pin1, unlike the FLAG-tagged wild-type CRTC1.

Then the effects of Pin1 on localizations of CRTC1 were examined. When LacZ was overexpressed, GFP-tagged CRTC1 was present in the cytosol and translocated to the nucleus in response to forskolin stimulation (supplemental Fig. 4*D*). This translocation was markedly inhibited by Pin1 overexpression (supplemental Fig. 4*D*).

CRTC2 Associated with Pin1 Did Not Bind to CREB—Formation of the CREB·CBP·CTRC complex, which binds to a CRE site, is critical for CRE transcriptional activation. We investigated whether or not the CREB·CBP·CRTC2·Pin1 complex can form, using the baculovirus and Sf9 cell overexpression system. When CRTC2 and CREB were both overexpressed in HepG2 or Sf9 cells, CREB was detected in the CRTC2 immunoprecipitate. Interestingly, the overexpression of Pin1 markedly reduced the association between CREB and CRTC2, in either HepG2 or Sf9 cells (Fig. 4, *A* and *B*).

Furthermore, the effect of Pin1 on the association between CRTC2 and 14-3-3 was investigated. In Sf9 cell lysates overexpressing CREB and CRTC2, both CRTC2 and endogenously expressed 14-3-3 protein were detected in anti-CREB immunoprecipitates (Fig. 4*C*). In the case of triple overexpressions of CRTC2, CREB, and GFP-tagged Pin1, CRTC2 and 14-3-3 were detectable in the GFP-tagged Pin1 immunoprecipitate (Fig. 4*D*).

Similar results were obtained in the HepG2 cells. The association between MEF-tagged CRTC2 and endogenously expressed 14-3-3 was not affected by the overexpression of Pin1 (supplemental Fig. 5*A*). In addition, Pin1 overexpression did not affect the phosphorylation level of Ser^{171}, responsible for the association with 14-3-3, in either basal or forskolin-stimulated conditions (supplemental Fig. 5*B*). These results suggest that Pin1-associated CRTC2 is capable of binding to 14-3-3 protein but not to CREB.

Pin1 Inhibits CRE Transcriptional Activity and Its Downstream PEPCK Expression—Subsequently, to elucidate the role of Pin1 in CRE transcriptional activity, the effects of Pin1 overexpression and Pin1 gene silencing using siRNA on the CRE and PEPCK luciferase assay, and PEPCK mRNA level were investigated in HepG2 cells (Fig. 5). The amount of overexpressed Pin1 was ~5 times that of endogenous Pin1 in HepG2 cells. Under these conditions, forskolin-induced transcriptional activity and PEPCK mRNA induction were significantly attenuated (Fig. 5, *A–C*). On the contrary, gene suppression of Pin1 using siRNA significantly enhanced these events (Fig. 5, *D–F*). In addition, suppressions of CRE-luciferase and PEPCK-luciferase activities by Pin1 overexpression were observed in immortalized human hepatocytes (supplemental Fig. 6) (25), suggesting that this mechanism is independent of the glucose sensitivity of the cell type. An inhibitory effect of Pin1 on CRE luciferase activity was observed when wild type or S171A CRTC2, but not S136A, was overexpressed, consistent with the results showing Pin1 to regulate the translocation of CRTC2 (supplemental Fig. 7). Thus, the Pin1 expression level was revealed to negatively regulate CRE transcriptional activity.

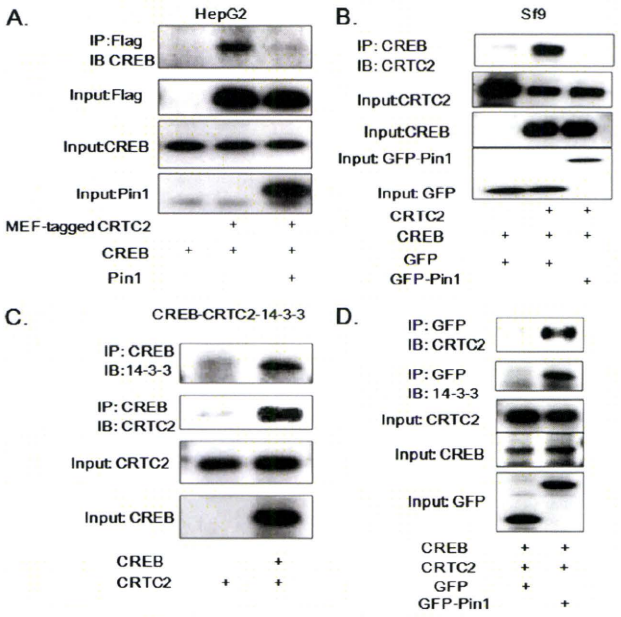

FIGURE 4. **Binding of Pin1 to CRTC2 inhibits the association between CREB and CRTC2 but not that between 14-3-3 and CRTC2.** *A*, MEF-tagged CRTC2, CREB, and Pin1 were overexpressed in HepG2 cells in the indicated combinations. The cell lysates were immunoprecipitated (*IP*) with anti-FLAG antibody and immunoblotted (*IB*) with anti-CREB antibody. *B*, CRTC2, CREB, and Pin1 were overexpressed in Sf9 cells in the indicated combinations. The cell lysates were immunoprecipitated with anti-CREB antibody and immunoblotted with anti-CRTC2 antibody. *C*, CREB and CRTC2 were overexpressed in Sf9 cells. The cell lysates were immunoprecipitated with anti-CREB antibody and immunoblotted with anti-14-3-3 protein antibody. *D*, CREB, CRTC2, and either GFP or GFP-Pin1 were overexpressed in Sf9 cells. The cell lysates were immunoprecipitated with anti-GFP antibody and immunoblotted with anti-CRTC2 or anti-14-3-3 protein antibody. Representative data from four independent experiments are shown.

Chromatin Immunoprecipitation Assay with Anti-CRTC2 and CREB Antibodies—Because Pin1-associated CRTC2 did not bind CREB, we performed a ChIP assay to investigate whether or not Pin1 affected recruitment of CRTC2 to cAMP-responsive elements upstream of PEPCK, NR4A2, and CGA genes (Fig. 5*G*). The PCR product obtained using the anti-CREB immunoprecipitate was unchanged regardless of forskolin stimulation or Pin1 overexpression. In contrast, the PCR product of the anti-CRTC2 immunoprecipitate was markedly increased by forskolin stimulation, and Pin1 overexpression abolished this increase. Forskolin stimulation induced CBP recruitment to the promoter as well as CRTC2, but Pin1 overexpression had no effect.

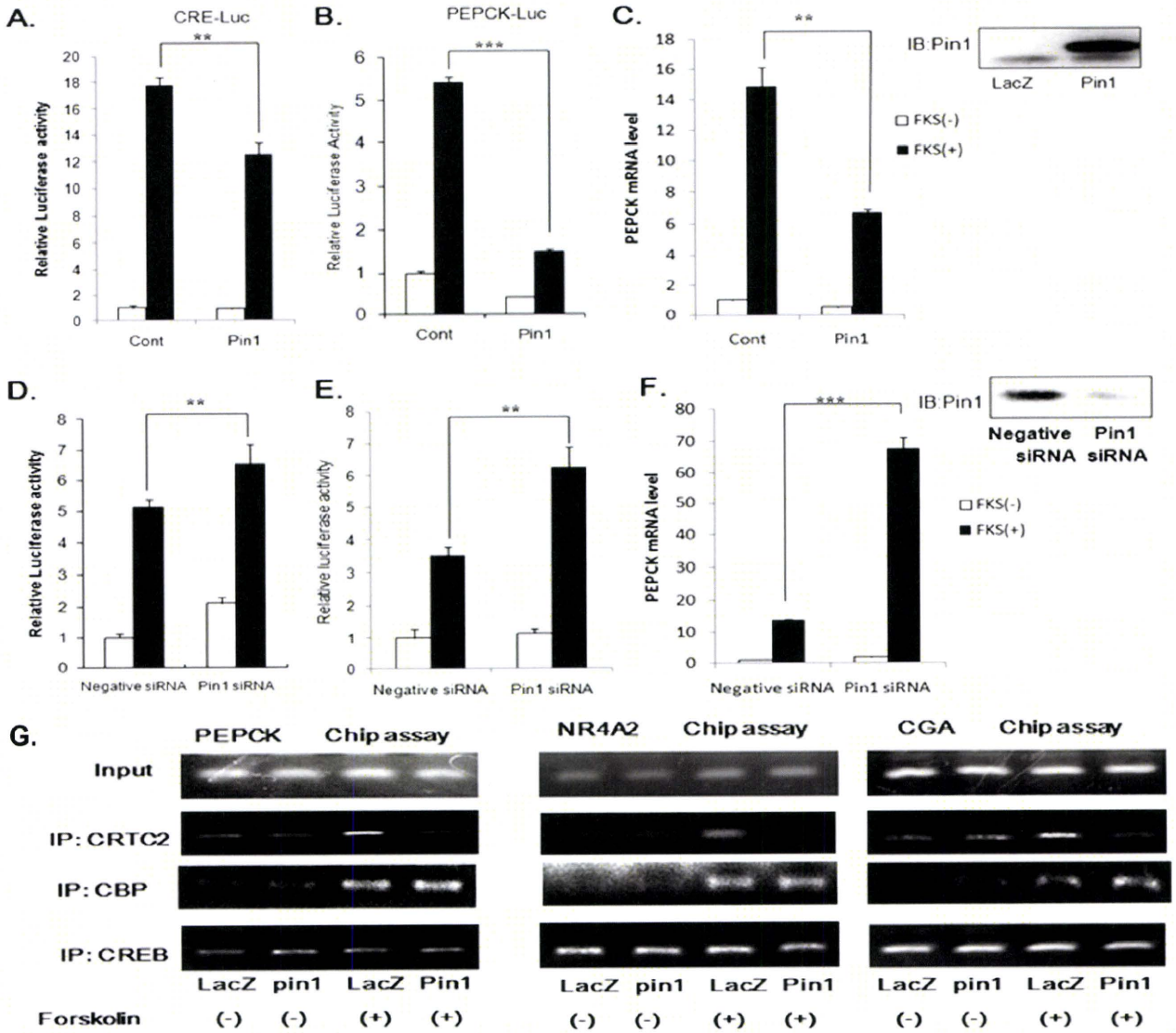

FIGURE 5. **Pin1 suppresses CRE luciferase activity and PEPCK mRNA level in HepG2 cells.** *A* and *B*, LacZ or Pin1 was overexpressed in HepG2 cells transfected with pTAL and pTAL-CRE or pTAL-PEPCK. *D* and *E*, these transfected HepG2 cells were treated with control siRNA or Pin1 siRNA. In two experiments, with and without forskolin stimulation for 6 h, the cell lysates from HepG2 cells were subjected to the luciferase assay. *C* and *F*, PEPCK mRNA levels were also measured. Representative data from four independent experiments are shown. **, $p < 0.01$ *versus* LacZ or negative siRNA. *G*, HepG2 cells overexpressing LacZ or Pin1 were subjected to the CHIP assay using anti-CRTC2, anti-CNP, or anti-CREB antibodies and primers corresponding to the PEPCK, NR4A2, and CGA promoter regions. Representative data from four independent experiments are shown. *IB*, immunoblot; *IP*, immunoprecipitation. *Error bars*, S.E.

Thus, it was suggested that CRTC2 associated with Pin1 was removed from CREB located in the CRE sequence in the PEPCK, NR4A2, and CGA promoter region.

Hepatic Pin1 Overexpression Reduces PEPCK Expression and Decreases Hyperglycemia in STZ-induced Diabetic Mice—CRTC2 is a major transcriptional co-activator for hepatic glucose regulation via its effects on PEPCK expression. Thus, we considered the possibility of the regulation of PEPCK expression by Pin1 in the liver, and an adenovirus expressing Pin1 was introduced into STZ-induced insulin-deficient diabetic mice. Due to the insulin deficiency, as reported previously, hepatic PEPCK mRNA and serum blood glucose levels were markedly increased in fed and fasted state, as compared with the control mice (Fig. 6). The adenovirus for Pin1 expression was injected intravenously, and 96 h later, overexpressed Pin1 was detected only in the liver (Fig. 6*A*) and not in other tissues. With Pin1 overexpression in the liver, the increased hepatic PEPCK mRNA level in STZ-mice was normalized, and blood glucose elevation was also partially but significantly reduced in both the fed and the fasting state (Fig. 6, *B–E*). Pin1 overexpression exerted the same effects on other CRE-dependent transcriptional genes, such as G6Pase, PGC-1a, and CPT-1. These findings revealed Pin1 to be a regulator of CRE-dependent transcriptional genes *in vivo*.

Pin1 Expression Is Low in Fasting State—Finally, we investigated the changes in Pin1 expressions under different nutrient condi-

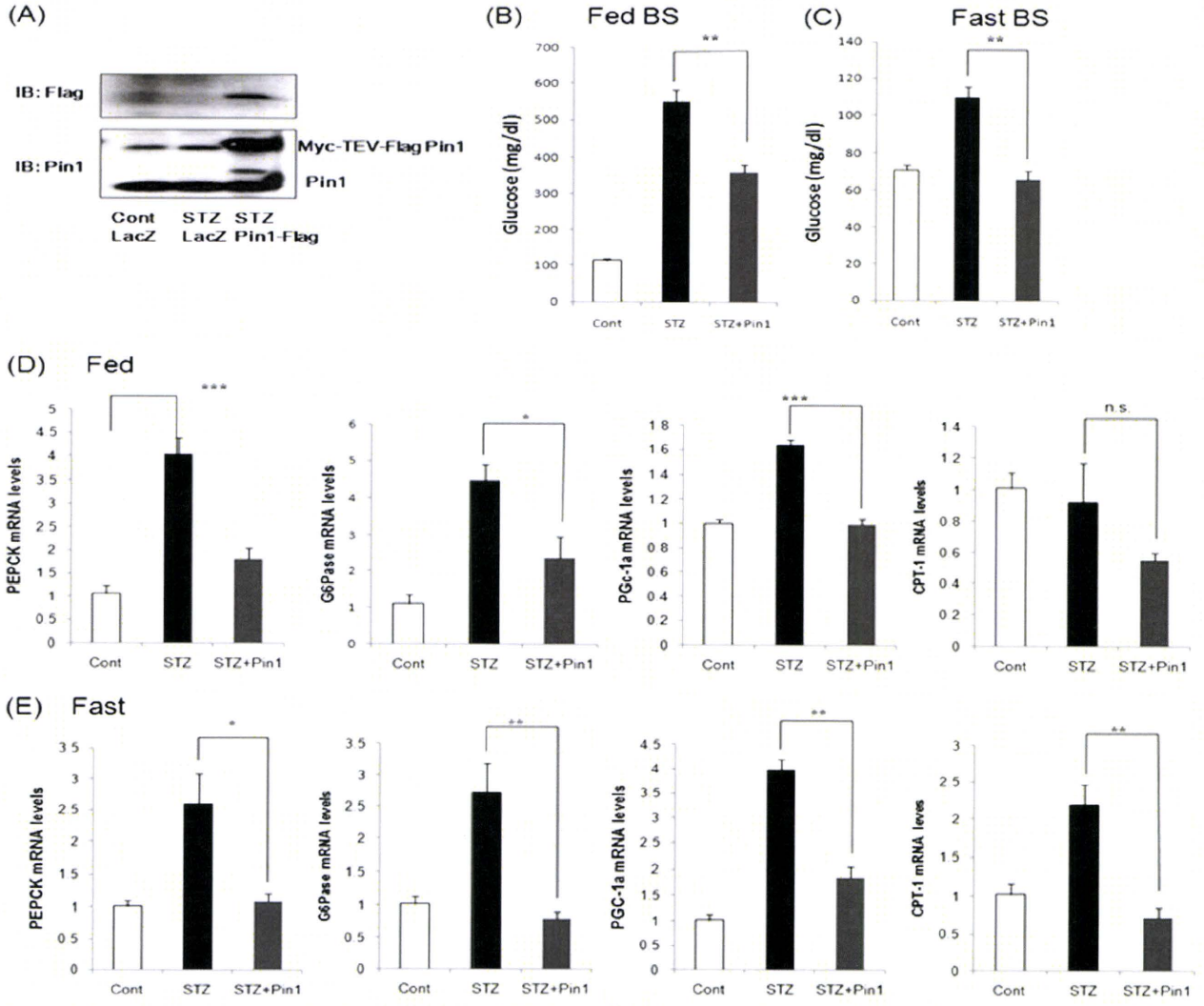

FIGURE 6. **Hepatic overexpression of Pin1 restored elevated CRE-dependent transcriptional genes and hyperglycemia in STZ-treated mice.** STZ-treated diabetic C57BL/6 male mice were injected with 2.5×10^7 plaque-forming units/g body weight of adenovirus containing β-galactosidase (*LacZ*) or FLAG-tagged Pin1 construct via the tail vein. *A*, immunoblotting of hepatic tissue lysates with anti-FLAG or anti-Pin1 antibody. *B* and *C*, serum glucose concentrations in fed and fasting states ($n = 6$, each group). *D* and *E*, CRE-dependent transcriptional gene mRNA levels in the liver. **, $p < 0.01$ *versus* STZ; ***, $p < 0.001$ *versus* STZ. *Error bars*, S.E.

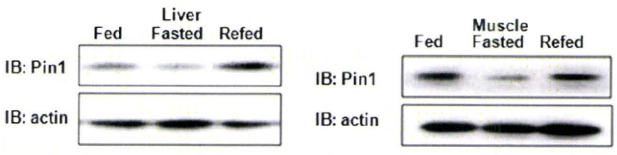

FIGURE 7. **Pin1 expression is regulated by nutrient conditions.** Mice were fed routinely, starved for 20 h, or refed for 4 h after a 20-h fast. Liver (*left*) and muscle (*right*) cell lysates were prepared and then immunoblotted with anti-Pin1 antibody. A representative immunoblot (*IB*) is shown in the *upper panel*.

tions. Interestingly, we found that the Pin1 expression level is low in the fasted state but is increased by feeding (Fig. 7). Thus, Pin1 expression appears to be regulated by nutrient conditions.

DISCUSSION

CRE transcriptional activity is enhanced through association of the CREB·CBP·CRTC complex on a CRE site. The co-activator of CREB termed the CRTC family consists of three isoforms, CRTC1, CRTC2, and CRTC3 (18). CRTC2 was reported to be important for the regulation of CRE transcriptional activity and its downstream PEPCK gene expression (20). Depletion of nuclear CRTC2 leads to the suppression of CRE transcriptional activity (20). Thus, both the subcellular localization of CRTC2 and CREB·CBP·CRTC complex formation are critical for CRE transcriptional activity. CRTC2 is reportedly phosphorylated by AMPK and SIK, and phosphorylated CRTC2 binds to 14-3-3 protein and is thereby shifted from the nucleus to the cytoplasm (21). The Montiminy group (16) has identified 12 independent phosphorylated serine residues on CRTC2 using tandem MS analysis. They demonstrated that PKA inhibits the activity of SIK and reduces Ser^{171} phosphorylation leading to binding with 14-3-3 protein and translocation to the cytosol (16). However, the importance of other phosphorylation sites identified in their study, such as Ser^{136} remains unknown.

In this study, it was demonstrated that Pin1 associates with the CRTC family of proteins consisting of CRTC1 and CRTC2. Because the portion of CRTC1 and CRTC2 responsible for the association with Pin1 is in the NLS domain, we considered the possibility that the binding of Pin1 to this portion would interrupt NLS function, resulting in their export from the nucleus. In fact, our observations using GFP-tagged CRTC1 and CRTC2 as well as staining of endogenous CRTC2 supported our hypothesis. On the other hand, gene silencing of Pin1 using siRNA markedly induced nuclear localization of CRTC2 when stimulated with forskolin. It is likely that altered localization of CTRC2 due to Pin1 takes place independently of the binding of 14-3-3 protein to CRTC2 because Pin1 overexpression affected neither the Ser^{171} phosphorylation level of CRTC2 nor the association with 14-3-3.

A further interesting issue is that CRTC2 associated with Pin1 did not bind to CREB. This phenomenon cannot be attributable to the different subcellular distributions of CREB, CBP, and CRTC because highly overexpressed CREB, CBP, and CRTC2 are present in the cytosol of Sf9 cells. Taken together, these observations indicate the association of Pin1 with CRTC2 to decrease the nuclear CBP·CRTC2·CREB complex via two mechanisms (*i.e.* the export of CRTC2 and interruption of the association between CRTC2 and CREB). Thus, the Pin1 expression level is a key factor regulating CRE transcriptional activity.

We investigated the effects of various kinase inhibitors on the association between CRTC2 and Pin1, using HepG2 cells, in an effort to identify the kinase that is involved in the phosphorylation of S136A on CRTC2. However, we were unable to obtain clear results. Although we did not discover which kinase(s) phosphorylates the Ser^{136} of CRTC2 responsible for the association with Pin1 in this study, high basal phosphorylation of Ser^{136} was already demonstrated in a previous report (16).

Prior studies have also shown that Pin1 expression generally correlates with cell proliferative potential in normal tissues (1, 26, 27) and is further up-regulated in many human cancers (28–31). In addition, interestingly, we noticed that the amount of Pin1 was higher in the fed than in the fasting state, in both liver and muscle. However, neither insulin nor forskolin has any effect on the expression of Pin1 in HepG2. Thus, the mechanism(s) involved in the altered expression of Pin1 remains unclear, although this is an important issue that merits further investigation.

In the liver, CRE transcriptional activity plays a critical role in gluconeogenesis (32–34). In addition, in the diabetic state, insufficient suppression of CRE transcriptional activity is regarded as a mechanism underlying hyperglycemia under fasted conditions (35). In the present study, our final experiment examined whether Pin1 overexpression might improve the hyperglycemia in insulin-deficient STZ-treated mice. In these mice, gluconeogenic enzymes, such as PEPCK, under the control of CRE transcriptional activity are reportedly up-regulated (20, 36, 37) due to insulin deficiency and the relatively increased effect of glucagon. The fact that Pin1 overexpression reduced the high PEPCK expression and its resultant fasting serum glucose elevation in STZ-treated mice suggests that the Pin1 expression level is involved in regulating glucose metabolism. Thus, an agent affecting Pin1 expression or activity may represent a novel therapeutic strategy for diabetes.

To date, numerous proteins have been identified as substrates of Pin1 (4, 5, 38). With the proline conformational change induced by Pin1, the structure and function of the target protein are modified, which affects protein stabilization, subcellular localization, phosphorylation, transcriptional activity, etc. In the case of CTRC2, both subcellular localization and the complex-forming function with CREB are affected.

Although we did not investigate the physiological effects occurring via CRTC1 induced by the association with Pin1, we did observe that Pin1 is highly expressed in the brain, whereas its enzymatic activity is blunted by oxidative stress modification that occurs in the early stages of Alzheimer disease (39). Although the physiological function of Pin1 in neurons remains largely unknown, numerous reports have implicated CRE transcriptional activity in brain function (40–42). Thus, further important evidence may be obtained from studies of Pin1 and CRTC1 in the brain or other tissues.

In summary, CRTC2 was identified as a new Pin1-binding protein. The CBP·CRTC2·CREB complex promotes gluconeogenesis. Pin1 binding to CRTC2 prevents this complex formation, thereby suppressing CRE transcriptional activity (supplemental Fig. 8). These findings indicate that Pin1 is a regulator of gluconeogenesis and may be a new target for diabetic therapy.

REFERENCES

1. Lu, K. P., Hanes, S. D., and Hunter, T. (1996) *Nature* **380,** 544–547
2. Lu, P. J., Wulf, G., Zhou, X. Z., Davies, P., and Lu, K. P. (1999) *Nature* **399,** 784–788
3. Pinton, P., Rimessi, A., Marchi, S., Orsini, F., Migliaccio, E., Giorgio, M., Contursi, C., Minucci, S., Mantovani, F., Wieckowski, M. R., Del Sal, G., Pelicci, P. G., and Rizzuto, R. (2007) *Science* **315,** 659–663
4. Takahashi, K., Uchida, C., Shin, R. W., Shimazaki, K., and Uchida, T. (2008) *Cell Mol. Life Sci.* **65,** 359–375
5. Wulf, G., Finn, G., Suizu, F., and Lu, K. P. (2005) *Nat. Cell Biol.* **7,** 435–441
6. Ranganathan, R., Lu, K. P., Hunter, T., and Noel, J. P. (1997) *Cell* **89,** 875–886
7. Schutkowski, M., Bernhardt, A., Zhou, X. Z., Shen, M., Reimer, U., Rahfeld, J. U., Lu, K. P., and Fischer, G. (1998) *Biochemistry* **37,** 5566–5575
8. Bittinger, M. A., McWhinnie, E., Meltzer, J., Iourgenko, V., Latario, B., Liu, X., Chen, C. H., Song, C., Garza, D., and Labow, M. (2004) *Curr. Biol.* **14,** 2156–2161
9. Dentin, R., Hedrick, S., Xie, J., Yates, J., 3rd, and Montminy, M. (2008) *Science* **319,** 1402–1405
10. He, L., Sabet, A., Djedjos, S., Miller, R., Sun, X., Hussain, M. A., Radovick, S., and Wondisford, F. E. (2009) *Cell* **137,** 635–646
11. Herzig, S., Long, F., Jhala, U. S., Hedrick, S., Quinn, R., Bauer, A., Rudolph, D., Schutz, G., Yoon, C., Puigserver, P., Spiegelman, B., and Montminy, M. (2001) *Nature* **413,** 179–183
12. Jansson, D., Ng, A. C., Fu, A., Depatie, C., Al Azzabi, M., and Screaton, R. A. (2008) *Proc. Natl. Acad. Sci. U.S.A.* **105,** 10161–10166
13. Lerner, R. G., Depatie, C., Rutter, G. A., Screaton, R. A., and Balthasar, N. (2009) *EMBO Rep.* **10,** 1175–1181
14. Liu, Y., Dentin, R., Chen, D., Hedrick, S., Ravnskjaer, K., Schenk, S., Milne, J., Meyers, D. J., Cole, P., Yates, J., 3rd, Olefsky, J., Guarente, L., and Montminy, M. (2008) *Nature* **456,** 269–273
15. Radhakrishnan, I., Pérez-Alvarado, G. C., Parker, D., Dyson, H. J., Montminy, M. R., and Wright, P. E. (1997) *Cell* **91,** 741–752
16. Screaton, R. A., Conkright, M. D., Katoh, Y., Best, J. L., Canettieri, G., Jeffries, S., Guzman, E., Niessen, S., Yates, J. R., 3rd, Takemori, H., Okamoto, M., and Montminy, M. (2004) *Cell* **119,** 61–74

17. Zhou, X. Y., Shibusawa, N., Naik, K., Porras, D., Temple, K., Ou, H., Kaihara, K., Roe, M. W., Brady, M. J., and Wondisford, F. E. (2004) *Nat. Med.* **10,** 633–637
18. Iourgenko, V., Zhang, W., Mickanin, C., Daly, I., Jiang, C., Hexham, J. M., Orth, A. P., Miraglia, L., Meltzer, J., Garza, D., Chirn, G. W., McWhinnie, E., Cohen, D., Skelton, J., Terry, R., Yu, Y., Bodian, D., Buxton, F. P., Zhu, J., Song, C., and Labow, M. A. (2003) *Proc. Natl. Acad. Sci. U.S.A.* **100,** 12147–12152
19. Wu, Z., Huang, X., Feng, Y., Handschin, C., Feng, Y., Gullicksen, P. S., Bare, O., Labow, M., Spiegelman, B., and Stevenson, S. C. (2006) *Proc. Natl. Acad. Sci. U.S.A.* **103,** 14379–14384
20. Dentin, R., Liu, Y., Koo, S. H., Hedrick, S., Vargas, T., Heredia, J., Yates, J., 3rd, and Montminy, M. (2007) *Nature* **449,** 366–369
21. Koo, S. H., Flechner, L., Qi, L., Zhang, X., Screaton, R. A., Jeffries, S., Hedrick, S., Xu, W., Boussouar, F., Brindle, P., Takemori, H., and Montminy, M. (2005) *Nature* **437,** 1109–1111
22. Sakoda, H., Gotoh, Y., Katagiri, H., Kurokawa, M., Ono, H., Onishi, Y., Anai, M., Ogihara, T., Fujishiro, M., Fukushima, Y., Abe, M., Shojima, N., Kikuchi, M., Oka, Y., Hirai, H., and Asano, T. (2003) *J. Biol. Chem.* **278,** 25802–25807
23. Xu, Y. X., and Manley, J. L. (2007) *Genes Dev.* **21,** 2950–2962
24. Shen, Z. J., Esnault, S., Schinzel, A., Borner, C., and Malter, J. S. (2009) *Nat. Immunol.* **10,** 257–265
25. Tontonoz, P., Hu, E., Devine, J., Beale, E. G., and Spiegelman, B. M. (1995) *Mol. Cell. Biol.* **15,** 351–357
26. Waki, K., Anno, K., Ono, T., Ide, T., Chayama, K., and Tahara, H. (2010) *Cancer Sci.* **101,** 1678–1685
27. Winkler, K. E., Swenson, K. I., Kornbluth, S., and Means, A. R. (2000) *Science* **287,** 1644–1647
28. Ryo, A., Nakamura, M., Wulf, G., Liou, Y. C., and Lu, K. P. (2001) *Nat. Cell Biol.* **3,** 793–801
29. Wulf, G. M., Ryo, A., Wulf, G. G., Lee, S. W., Niu, T., Petkova, V., and Lu, K. P. (2001) *EMBO J.* **20,** 3459–3472
30. Yeh, E., Cunningham, M., Arnold, H., Chasse, D., Monteith, T., Ivaldi, G., Hahn, W. C., Stukenberg, P. T., Shenolikar, S., Uchida, T., Counter, C. M., Nevins, J. R., Means, A. R., and Sears, R. (2004) *Nat. Cell Biol.* **6,** 308–318
31. Zheng, H., You, H., Zhou, X. Z., Murray, S. A., Uchida, T., Wulf, G., Gu, L., Tang, X., Lu, K. P., and Xiao, Z. X. (2002) *Nature* **419,** 849–853
32. Erion, D. M., Ignatova, I. D., Yonemitsu, S., Nagai, Y., Chatterjee, P., Weismann, D., Hsiao, J. J., Zhang, D., Iwasaki, T., Stark, R., Flannery, C., Kahn, M., Carmean, C. M., Yu, X. X., Murray, S. F., Bhanot, S., Monia, B. P., Cline, G. W., Samuel, V. T., and Shulman, G. I. (2009) *Cell Metab.* **10,** 499–506
33. Rhee, J., Inoue, Y., Yoon, J. C., Puigserver, P., Fan, M., Gonzalez, F. J., and Spiegelman, B. M. (2003) *Proc. Natl. Acad. Sci. U.S.A.* **100,** 4012–4017
34. Rodgers, J. T., Lerin, C., Haas, W., Gygi, S. P., Spiegelman, B. M., and Puigserver, P. (2005) *Nature* **434,** 113–118
35. Yoon, J. C., Puigserver, P., Chen, G., Donovan, J., Wu, Z., Rhee, J., Adelmant, G., Stafford, J., Kahn, C. R., Granner, D. K., Newgard, C. B., and Spiegelman, B. M. (2001) *Nature* **413,** 131–138
36. Clément, S., Krause, U., Desmedt, F., Tanti, J. F., Behrends, J., Pesesse, X., Sasaki, T., Penninger, J., Doherty, M., Malaisse, W., Dumont, J. E., Le Marchand-Brustel, Y., Erneux, C., Hue, L., and Schurmans, S. (2001) *Nature* **409,** 92–97
37. Fisher, S. J., and Kahn, C. R. (2003) *J. Clin. Invest.* **111,** 463–468
38. Ryo, A., Suizu, F., Yoshida, Y., Perrem, K., Liou, Y. C., Wulf, G., Rottapel, R., Yamaoka, S., and Lu, K. P. (2003) *Mol Cell.* **12,** 1413–1426
39. Sultana, R., Boyd-Kimball, D., Poon, H. F., Cai, J., Pierce, W. M., Klein, J. B., Markesbery, W. R., Zhou, X. Z., Lu, K. P., and Butterfield, D. A. (2006) *Neurobiol. Aging* **27,** 918–925
40. Bito, H., Deisseroth, K., and Tsien, R. W. (1996) *Cell* **87,** 1203–1214
41. Nibuya, M., Nestler, E. J., and Duman, R. S. (1996) *J. Neurosci.* **16,** 2365–2372
42. Tao, X., Finkbeiner, S., Arnold, D. B., Shaywitz, A. J., and Greenberg, M. E. (1998) *Neuron* **20,** 709–726